# LOS ALAMOS SCIENTIFIC LABORATORY

OF THE UNIVERSITY OF CALIFORNIA

LOS ALAMOS, NEW MEXICO

CONTRACT W-7405-ENG.36 WITH THE
U.S. ATOMIC ENERGY COMMISSION

[redacted] UNCLASSIFIED

UNCLASSIFIED

LOS ALAMOS SCIENTIFIC LABORATORY
of the
UNIVERSITY OF CALIFORNIA

Report written:
December 1954



LA-1863
C.3
This document consists of 42 pages
[redacted]

# EMISSION PROBABILITIES OF PROMPT NEUTRONS FROM SPONTANEOUS AND NEUTRON-INDUCED FISSION

by
R. B. Leachman





PHYSICS AND MATHEMATICS
(M-3679, 15th edition)

[redacted] UNCLASSIFIED

UNCLASSIFIED

[redacted]

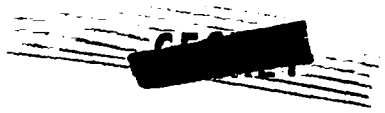



PHYSICS AND MATHEMATICS
(M-3679, 15th edition)



Report distributed: APR 8 1955

LA-1863

| | |
|---|---|
| Los Alamos Report Library | 1-20 |
| AF Plant Representative, Burbank | 21 |
| AF Plant Representative, Seattle | 22 |
| AF Plant Representative, Wood-Ridge | 23 |
| American Machine and Foundry Company | 24 |
| ANP Project Office, Fort Worth | 25 |
| Argonne National Laboratory | 26-30 |
| Armed Forces Special Weapons Project (Sandia) | 31 |
| Army Chemical Center | 32 |
| Atomic Energy Commission, Washington | 33-35 |
| Babcock and Wilcox Company | 36 |
| Battelle Memorial Institute | 37 |
| Bendix Aviation Corporation | 38 |
| Brookhaven National Laboratory | 39-41 |
| Bureau of Ships | 42 |
| Carbide and Carbon Chemicals Company (C-31 Plant) | 43 |
| Carbide and Carbon Chemicals Company (K-25 Plant) | 44-45 |
| Carbide and Carbon Chemicals Company (ORNL) | 46-51 |
| Chicago Patent Group | 52 |
| Chief of Naval Research | 53 |
| Columbia University (Havens) | 54 |
| Commonwealth Edison Company | 55-56 |
| Department of the Navy--Op-362 | 57 |
| Detroit Edison Company | 58 |
| Directorate of Research (WADC) | 59 |
| duPont Company, Augusta | 60-62 |
| Duquesne Light Company | 63 |
| Foster Wheeler Company | 64 |
| General Electric Company (ANPD) | 65-68 |
| General Electric Company (APS) | 69 |
| General Electric Company, Richland | 70-77 |
| Goodyear Atomic Corporation | 78-79 |
| Hanford Operations Office | 80 |
| Headquarters, Air Force Special Weapons Center | 81 |
| Iowa State College | 82 |
| Knolls Atomic Power Laboratory | 83-86 |
| Monsanto Chemical Company | 87 |
| Mound Laboratory | 88-89 |
| National Advisory Committee for Aeronautics, Cleveland | 90 |
| National Bureau of Standards | 91 |
| Naval Medical Research Institute | 92 |
| Naval Research Laboratory | 93-94 |
| New Brunswick Laboratory | 95 |
| Newport News Shipbuilding and Dry Dock Company | 96 |
| New York Operations Office | 97 |
| North American Aviation, Inc. | 98-100 |
| Nuclear Development Associates, Inc. | 101 |
| Nuclear Metals, Inc. | 102 |
| Pacific Northwest Power Group | 103 |
| Patent Branch, Washington | 104 |
| Phillips Petroleum Company (NRTS) | 105-108 |
| Powerplant Laboratory (WADC) | 109 |
| Pratt & Whitney Aircraft Division (Fox Project) | 110 |
| Sandia Corporation | 111 |
| Tennessee Valley Authority (Dean) | 112 |
| USAF Project RAND | 113 |
| U. S. Naval Radiological Defense Laboratory | 114 |
| UCLA Medical Research Laboratory | 115 |
| University of California Radiation Laboratory, Berkeley | 116-118 |
| University of California Radiation Laboratory, Livermore | 119-121 |
| University of Rochester | 122-123 |
| Vitro Engineering Division | 124 |
| Walter Kidde Nuclear Laboratories, Inc. | 125 |
| Bettis Plant (WAPD) | 126-129 |
| Yale University | 130 |
| Kaiser Engineers | 131 |
| U. S. Naval Postgraduate School | 132 |
| Engineer Research and Development Laboratories | 133 |
| Pennsylvania Power and Light Company | 134 |
| Westinghouse Electric Corporation (IAPG) | 135 |
| Technical Information Service, Oak Ridge | 136-150 |





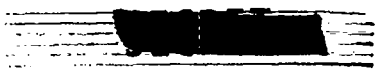

## ABSTRACT

A method is developed for using the relatively easily measured fission parameters, together with the mass equation of fission and the evaporation model of the nucleus, to determine the emission probabilities of the fission neutrons. The distribution of the kinetic energies of the fragment pairs enters into these calculations in a sensitive manner. Neutron emission probabilities are computed for the fission of the compound nuclei $U^{234}$, $U^{236}$, and $Pu^{240}$, for which cases reasonably adequate data on the fragment pair energies are available. Although the corresponding data for the fission of the compound nuclei $Th^{233}$, $U^{238}$, and $U^{239}$ are considerably poorer, neutron emission probabilities are also computed.

The calculated results from this method are in good agreement with direct measurements of fission neutrons.



## ACKNOWLEDGMENTS

The author wishes to acknowledge the suggestions made by C. D. Coryell on the mass surface, V. F. Weisskopf on the neutron temperatures, H. H. Barschall and R. G. Thomas on the evaporation model, and J. A. Wheeler on the solution of the integral equations. Also, the considerable work done by M. T. Goldstein and I. J. Cherry on the calculations is appreciated.

CONTENTS



TABLES

[redacted]

TABLES (Continued)



ILLUSTRATIONS





[redacted]

## INTRODUCTION

The emission probabilities of fission neutrons are of interest in both reactor and weapons work. Experimental determinations of even the average number of neutrons $\overline{\nu}$ emitted per fission have been handicapped by the variation in the detection efficiencies of neutron detectors with neutron energy and the difficulty of determining these efficiencies. Also, because of the low detection efficiencies, it has been particularly difficult to make absolute measurements of the variation in the number of fission neutrons emitted in each fission event. Until the recent development of the large volume scintillation tanks containing cadmium, the neutron detectors used for fission neutrons had low efficiencies, usually of only a few percent. Such low detection efficiency made multiplicity measurements of fission neutron emission particularly difficult.

As a result of these experimental difficulties there have existed large uncertainties in $\overline{\nu}$, especially for fission induced by neutrons in the vicinity of 1 to 14 Mev, in which region the detector must be shielded from the neutrons inducing fission. The present calculations are an effort to use the more easily measured parameters of fission to calculate neutron emission probabilities for several fissile nuclides at several excitation energies inducing fission. These more easily measured parameters are the masses of the fission products as obtained from mass spectrographic measurements and the energy surface from energy systematics, together with the measured kinetic energy of the fission products. These quantities are used in the mass equation of fission to determine the excitation energy of the fission products. This excitation energy is used with the evaporation model of the nucleus to compute neutron emission probabilities of fission.

In the following analysis these quantities will all be used in their probability distributions and all distributions will be normalized to unity. In the initial analyses that were made, the calculations were by graphic means and by hand calculations. However, the bulk of the data that have been compiled in this report is the result of rather extensive calculations on the IBM 701.

## BASIC ASSUMPTIONS

Three basic assumptions are used in the present method. These assumptions are:

(a) The basic determination of the kinetic energy of the fission products is the Coulomb

energy of repulsion of the nuclear charges of the two fission products from binary fission.

(b) A semi-empirical mass surface, including the effects of shell edges, can be used to obtain masses of atoms for which mass spectrographic measurements have not been made and also can be used to obtain neutron binding energies for nuclei for which the binding energies have not been measured.

(c) A simple form of the evaporation model of the nucleus can be used to calculate the emission probabilities of neutrons for the primary fission products as a function of the excitation energy of these nuclides.

Although complete investigations have not been made of these three assumptions, particularly of (b) and (c), the available data do indicate that all three are reasonable assumptions.

In particular, the Coulomb energy assumption in (a) has been confirmed by the kinetic energy measurements of fission products for rather wide variations of excitation inducing fission. Both Wahl[1] and Friedland[2] have measured the kinetic energy of the fission products of 14-Mev neutron induced fission of $U^{235}$ and have found essentially the same average kinetic as for thermal-neutron induced fission. In addition, Wahl has found the same condition existing for high- and low-energy neutron induced fission of both $Pu^{239}$ and $U^{238}$. Similarly, Segrè and Weigand[3] have found the same kinetic energy of the fission products for spontaneous fission of $Pu^{240}$ and for thermal-neutron induced fission of $Pu^{239}$. An independent confirmation of the Coulomb origin of the kinetic energy of the fission products is provided by the analysis of this energy as a function of the mass ratio of the fission products by Fong.[4] Fong has found that, except for an anomalous effect in the region of symmetrical fission, the average kinetic energy as a function of mass ratio is of Coulomb origin.

It should be pointed out that the Coulomb origin of the fission energy can explain the variation in the kinetic energy of the fission products for a particular mass ratio only if some assumptions of variable breaking distances for fissioning nuclei are made. However, such assumptions do not invalidate the analysis being made.

The semi-empirical mass surface has been discussed by many authors and has received a thorough analysis by Coryell.[5] Coryell has shown the effect of closed nuclear shells on

---

[1] J. S. Wahl, Phys. Rev. 95, 126 (1954).

[2] S. S. Friedland, Phys. Rev. 84, 75 (1951).

[3] E. Segrè and C. Weigand, Phys. Rev. 94, 157 (1954).

[4] P. Fong, A Theory of Fission (unpublished).

[5] C. D. Coryell, Ann. Rev. Nuclear Sci. 2, 305 (1953).

[redacted]

various parameters in the expression for this mass surface and has demonstrated that the parabolic shape applies for given values of mass number A over the range of nuclear charge Z that has been measured. Unfortunately, the shape of the mass surface has not been measured as far from the stable nuclear charge as the neutron-rich primary fission products are found.

The validity of the semi-empirical mass surface to compute neutron binding energies has been demonstrated[6] by comparing these computed energies with measured binding energies. Although a mass surface that did not include the effects of closed nuclear shells was used, the results of these analyses showed that satisfactory agreement between the measured and calculated binding energies would be obtained if the effects of nuclear shells were included. However, once again, these comparisons were for nuclides considerably nearer stable Z than are the primary fission products.

The evaporation model of the nucleus as described by Blatt and Weisskopf[7] has been tested by comparing results from it with experimental results of particle emission in several types of experiments. Although this model provides a convenient picture of particle emission, Cohen,[8] in a summary of the comparisons with experimental results, has shown that the model has limited accuracy. Cohen has shown the need for a nuclear temperature dependence on the amount of the excitation and the method of formation of the compound nucleus. Again, the experimental tests of this model have been made only with nuclides much nearer stable Z than are the primary fission products.

## MASS EQUATION OF FISSION

The basic mass equation of fission for $U^{236}$ is

$$M(U^{236}) + E_b = M(A^L, \delta^L, Z^L) + M(A^H, \delta^H, Z^H) + E_C + E_X. \quad (1)$$

This equation is written in units of Mev where the conversion between the masses M and energy is by the factor 931.15 Mev/mass unit. Since the equation is for the primary fission products before neutron emission, $A^H + A^L = 236$ and $Z^L + Z^H = 92$ are required for this case of $U^{236}$ fission to conserve nucleon number and charge number. Here and throughout

[6] J. A. Harvey, Phys. Rev. 81, 353 (1951) and Sher, Halpern, and Mann, Phys. Rev. 84, 387 1951).

[7] J. M. Blatt and V. F. Weisskopf, Theoretical Nuclear Physics, John Wiley and Sons, New York, 1952.

[8] B. L. Cohen, Phys. Rev. 92, 1245 (1953).



[redacted]

this report, the superscripts L and H refer to the light and heavy fragments, respectively. In Eq. 1, $\delta$ is the even-odd parameter discussed by Coryell.[5] The masses of the fission products are the ground state masses of these unstable fission products. Furthermore, $E_C$ is the Coulomb energy of the fission products; $E_X$ is the sum of the excitation energies of these primary fission products; and $E_b$ is the bias energy inducing fission with reference to spontaneous fission, where $E_b = E_n + B_n$.[9] The binding energy $B_n$ is that of a neutron to the nucleus undergoing fission and $E_n$ is the energy of the neutron inducing fission.

The masses in this mass equation of fission are based on masses from mass spectrographic data. These mass spectrographic measurements are usually of about 1-Mev uncertainty and the masses in the fission product region are accurate relative to the masses of the fissioning nuclei because of the method of comparison with the lighter elements used in the mass measurements of the heavy, fissionable nuclei. The masses of the fissionable nuclei are from the compilation of Huizenga and Magnusson.[10] The masses of the stable atoms in the region of the fission products were obtained from the mass measurements of Duckworth et al.[11] and of the Minnesota group.[12] These mass measurements are shown in Fig. 1, after having been converted to masses of odd A and to the non-integer stable nuclear charge for that mass number. The conversion to odd A is by the $\delta$ values of Fermi.[13] The conversion to the stable nuclear charge is by the stable charge values and parabolic surface constants of Coryell.[5] The conversion from these masses for the valley of the mass surface to the masses of the primary fission products was made by the same conversion parameters.

---

[9] J. L. Fowler (Oak Ridge National Laboratory Report ORNL-1374, December 1952) first pointed out that the Coulomb energy of fission is constant, and thus the excitation energy of the fragments increases as the energy of the neutron inducing fission.

[10] J. R. Huizenga and L. B. Magnusson, Argonne National Laboratory Report ANL-5158, November 1953.

[11] E. M. Pennington and H. E. Duckworth, Can. J. Phys. 32, 808 (1954); B. J. Hogg and H. E. Duckworth, Can. J. Phys. 32, 65 (1954) and 31, 942 (1953); H. E. Duckworth and R. S. Preston, Phys. Rev. 82, 468 (1951) and 79, 402 (1950); Duckworth, Woodcock, and Preston, Phys. Rev. 78, 479 (1950); Duckworth, Preston, and Woodcock, Phys. Rev. 79, 188 (1950); Duckworth, Kegley, Olson and Stanford, Phys. Rev. 83, 1114 (1951); C. L. Kegley and H. E. Duckworth, Phys. Rev. 83, 229 (1951); and B. J. Hogg and H. E. Duckworth, Can. J. Phys. 30, 637 (1952).

[12] Collins, Nier, and W. H. Johnson, Jr., Phys. Rev. 86, 408 (1952); Collins, Johnson, Jr., and Nier, Phys. Rev. 94, 398 (1954); and R. E. Halsted, Phys. Rev. 88, 666 (1952).

[13] E. Fermi, Nuclear Physics, notes compiled by J. Orear, A. H. Rosenfeld, and R. A. Schluter, University of Chicago Press, Chicago, 1949.

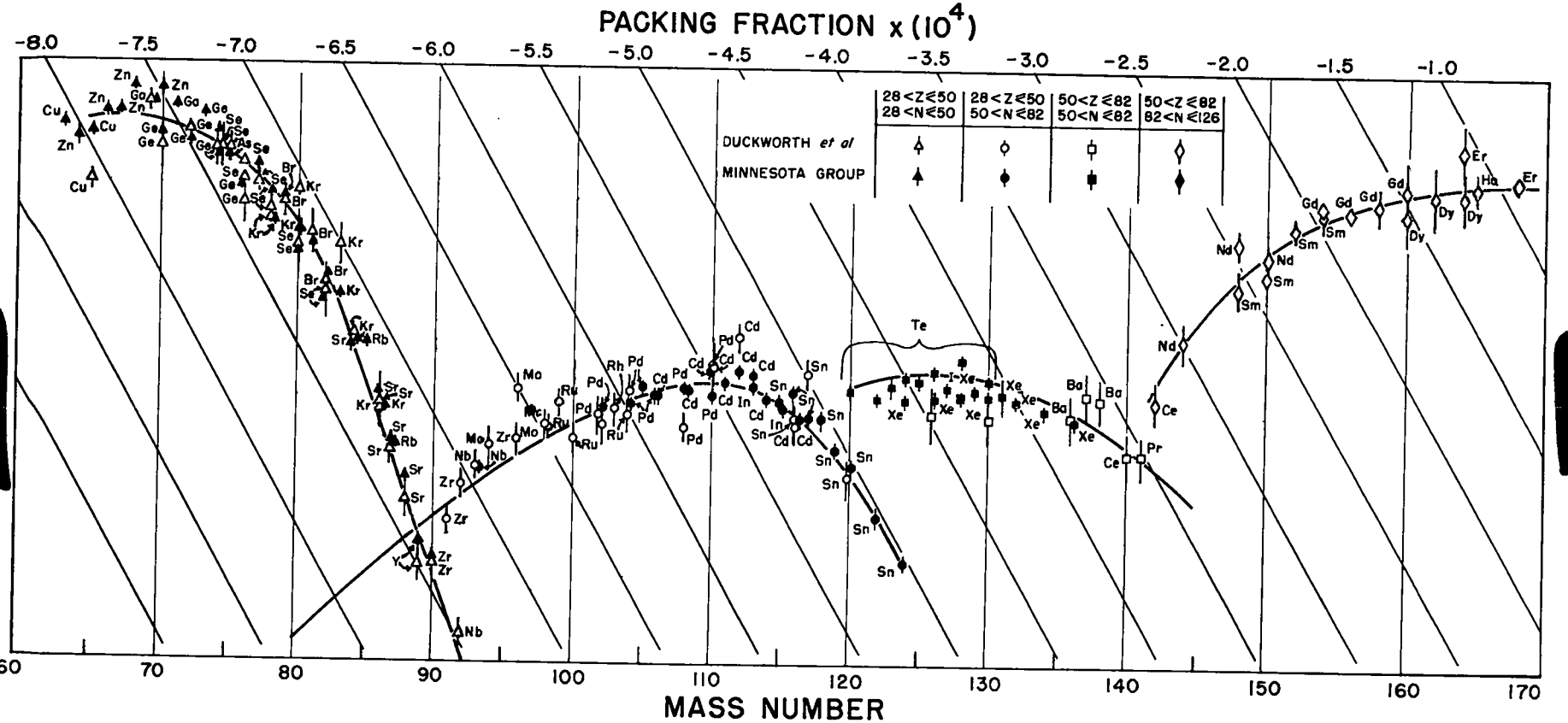


Fig. 1. Masses of the valley of the semi-empirical mass surface. Data are mass spectrographic data converted to odd A and to the non-integer charge Z that, for each value of A, corresponds to the valley of the mass surface.


APPROVED FOR PUBLIC RELEASE

## DISTRIBUTION IN FISSION FRAGMENT MASS

It has been shown[14] that for fission induced by excitations of less than about 40 Mev, definite peaks exist in the mass distribution of the fission yield of the various fissioning nuclides that are all characterized by a low probability of fission for symmetrical fission. As is readily seen in Eq. 1, the sum of the fission energies will be dependent upon the masses of the fission products. This is emphasized by rewriting Eq. 1 as

$$E_C + E_X = \phi(\delta, R_m, R_Z). \tag{2}$$

Further, the yield for symmetrical fission is found to increase as the energy inducing fission $E_b$ increases.[15] However, in all cases being investigated, the yield in the symmetrical fission region is sufficiently low that this change of yield may be neglected.

In the analysis for each nucleus undergoing fission, the mass yield is divided into three groups of mass ratio $R_m$. In each case the division of the mass yield is chosen such that one division is at the 82-neutron shell. The spike in the mass yield curve at this shell as found by mass spectrographic means has not been included, but instead the smooth mass yield curve is used. The neutron emission characteristics of each group of fission masses for each fissioning nuclei are investigated separately and then combined to determine the neutron emission characteristic of that fissioning nucleus.

## DISTRIBUTION IN NUCLEAR CHARGE

The nuclear charge is seen by Eqs. 1 and 2 to be a parameter in the determination of the energies of fission. Fortunately for simplicity of calculation, the distribution in the nuclear charge for each mass ratio of fission is sharp, and little error is induced by using only the most probable nuclear charge.

Glendenin[16] has investigated the nuclear charge of the fission products after neutron emission as a function of the stable nuclear charge of that mass of fission product. More recently Pappas[17] has included the effect of nuclear shells on the line of nuclear charge

---

[14] C. D. Coryell and N. Sugarman, eds., Radiochemical Studies: The Fission Products, Appendix B, Div. IV, Vol. 9, National Nuclear Energy Series, McGraw-Hill Book Company, Inc., New York, 1951.

[15] R. A. Schmitt and N. Sugarman, Phys. Rev. 95, 1260 (1954).

[16] Reference 14, Paper 52.

[17] A. C. Pappas, Massachusetts Institute of Technology, Laboratory for Nuclear Science Technical Report No. 63, 1953.

stability in such an analysis of the charge of the fission products. It is seen from such analyses that the distribution in the nuclear charge is about two charge units wide at half maximum.

In Fig. 2 is shown the variation of the fission energies as a function of the nuclear charge for fission of $U^{236}$ into the most probable fission mass ratio. It is seen from this figure that the roughly 4-Mev width of the excitation energy distribution caused by the charge distribution is small compared to the roughly 15-Mev widths of the excitation energy distributions to be used. Consequently, only one nuclear charge, the most probable nuclear charge, is used in the calculations for each mass ratio of fission.

## DISTRIBUTION IN KINETIC ENERGY

The distributions $I(E_I)$ in the measured total kinetic energy of fission, $E_I$, are obtained from the double ionization chamber measurements of the kinetic energy made by Brunton and Hanna[18] and Brunton and Thompson.[19] Through the use of the momentum equation which applies for binary fission, these measurements of the kinetic energy of the fission pairs by the ionization are expressed in terms of the probability as a function of the mass ratio $R_m$ of fission. Thus, it is possible to determine the distribution in the total kinetic energy of the fragment pairs for each mass ratio being considered.

A comparison[20] of the mass distribution obtained in a similar manner with the mass distribution obtained by radiochemical means[14] has demonstrated the existence of a dispersion in the measurement of energy by ionization of approximately 8-Mev full width at half maximum for each fragment and thus of approximately 11.4-Mev full width at half maximum for the total kinetic energy of the fragment pairs. Similarly, a comparison[21] of the directly measured velocities of fission fragments with the velocities inferred from the ionization chamber measurements demonstrated a dispersion of approximately 9 Mev for each fragment. Further, this comparison of velocities showed that the ionization chamber measurements of the kinetic energies $I_I^L$ and $E_I^H$ are low by 5.7 and 6.7 Mev, respectively. The energy that is not observed as ionization has been explained[22] in terms of the ionization defects of fission fragments.

---

[18] D. C. Brunton and G. C. Hanna, Can. J. Research A28, 190 (1950).

[19] D. C. Brunton and W. B. Thompson, Can. J. Research A28, 498 (1950).

[20] R. B. Leachman, Phys. Rev. 83, 17 (1951).

[21] R. B. Leachman, Phys. Rev. 87, 444 (1952).

[22] J. K. Knipp and R. C. Ling, Phys. Rev. 82, 30 (1951).

[redacted]

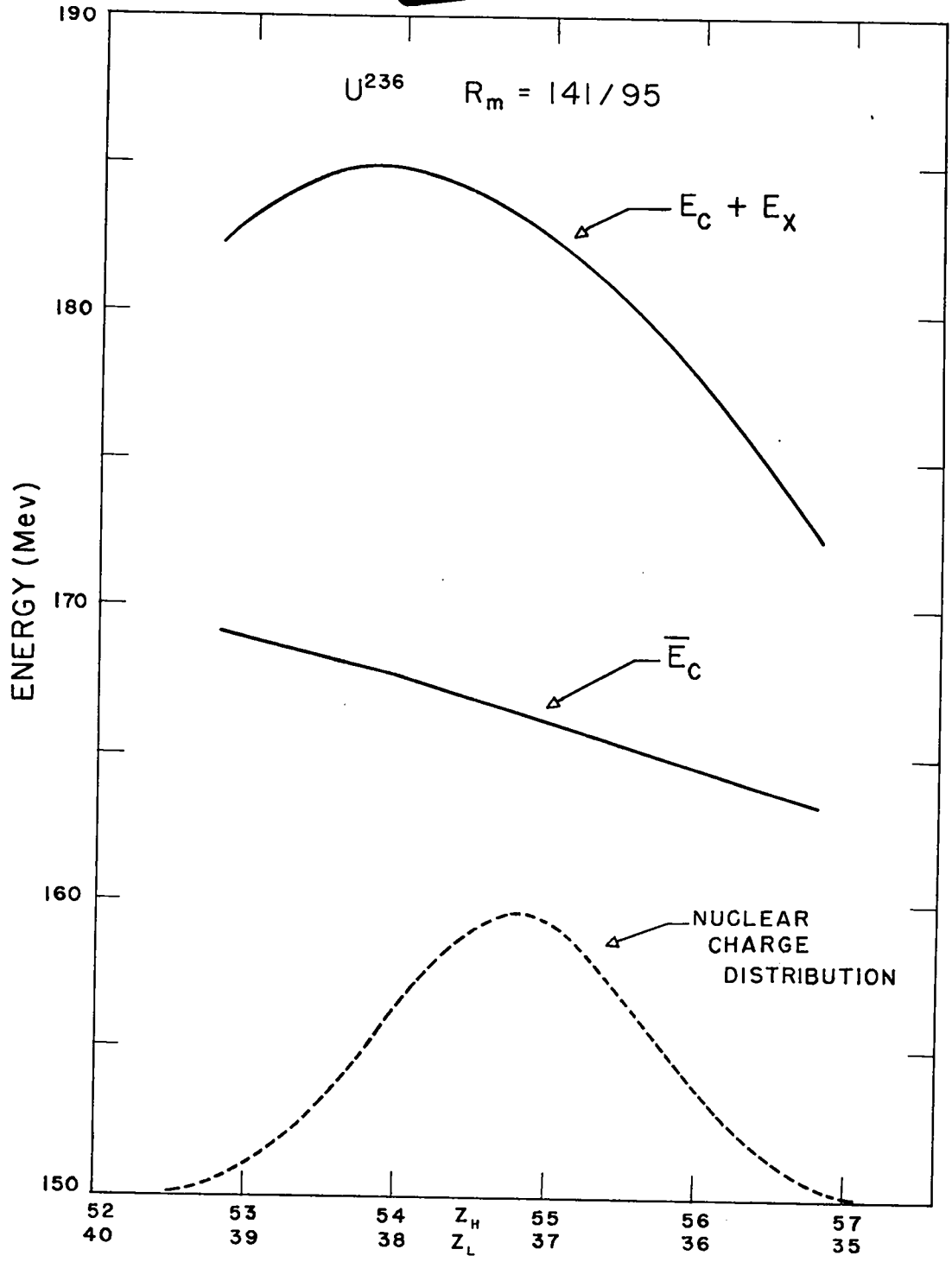


Fig. 2. Fission energy dependence upon nuclear charge ratio for the most probable mass ratio of $U^{236}$ fission. The Coulomb energy is normalized to the most probable measured kinetic energy (corrected for ionization defect) at the most probable charge ratio. The variation with nuclear charge is calculated on the basis of a Coulomb origin. The sum $E_C + E_X$ is calculated from Eq. 1. The nuclear charge distribution is from Glendenin.[16]



[redacted]

[redacted]

In Fig. 3 is shown a typical distribution $I(E_I, R_m)$ as obtained by Brunton and Hanna[18] for fission of the compound nucleus $U^{236}$ at the most probable mass ratio.

This distribution contains the distribution in the ratio of the nuclear charge $R_Z$. For a rigorous treatment of the emission probabilities a distribution of energies as a function also of the ratio of nuclear charge $R_Z$ is needed. However, calculations from the data in Fig. 2 show the distribution in the kinetic energy is changed only by a very small amount by the effects of the distribution in the nuclear charge.

To convert the measured distributions $I(E_I, R_m^{\cdot})$ to the distribution in the true kinetic energy of fission $C(E_C, R_m)$, it is necessary to unfold the effects of the dispersion and transpose by the amount of the ionization defects in the ionization chamber measurements of energy to obtain this true, or Coulomb, energy of fission. Unfortunately, the comparisons[20,21] of fission parameters are not sufficiently sensitive to determine both the breadth and the shape of the dispersion functions that lead to the experimental data. However, these analyses do indicate that a Gaussian shaped dispersion does satisfactorily fit the data. For ease of calculations, Gaussian dispersions are used in the present analysis.

The expression for the dispersion in the data obtained from ionization chamber measurements is

$$D_1(E_I, E_C) \propto \exp\left[-\left(\frac{E_I + 12.4 - E_C}{u_1}\right)^2\right] . \tag{3}$$

The 12.4-Mev constant in the exponential is the ionization defect term and $u_1$ is the dispersion width. It is seen from Fig. 2 that the dispersion introduced by the distribution in the nuclear charge is of approximately Gaussian shape and thus this dispersion similarly is expressed as a Gaussian in

$$D_2(E_I, E_C) \propto \exp\left[-\left(\frac{E_I + 12.4 - E_C}{u_2}\right)^2\right] . \tag{4}$$

The term $u_2$ in the exponential is the width of this dispersion. It can readily be shown that the combined effect of these two dispersions is itself a Gaussian dispersion. Equation 5,

$$D(E_I, E_C) \propto \exp\left[-\left(\frac{E_I + 12.4 - E_C}{u}\right)^2\right] , \tag{5}$$

is the expression for this combined dispersion, where u is the combined width. In the bulk of the calculations, 7.2 Mev is taken as the value for u. This is obtained by weighting the



[redacted]

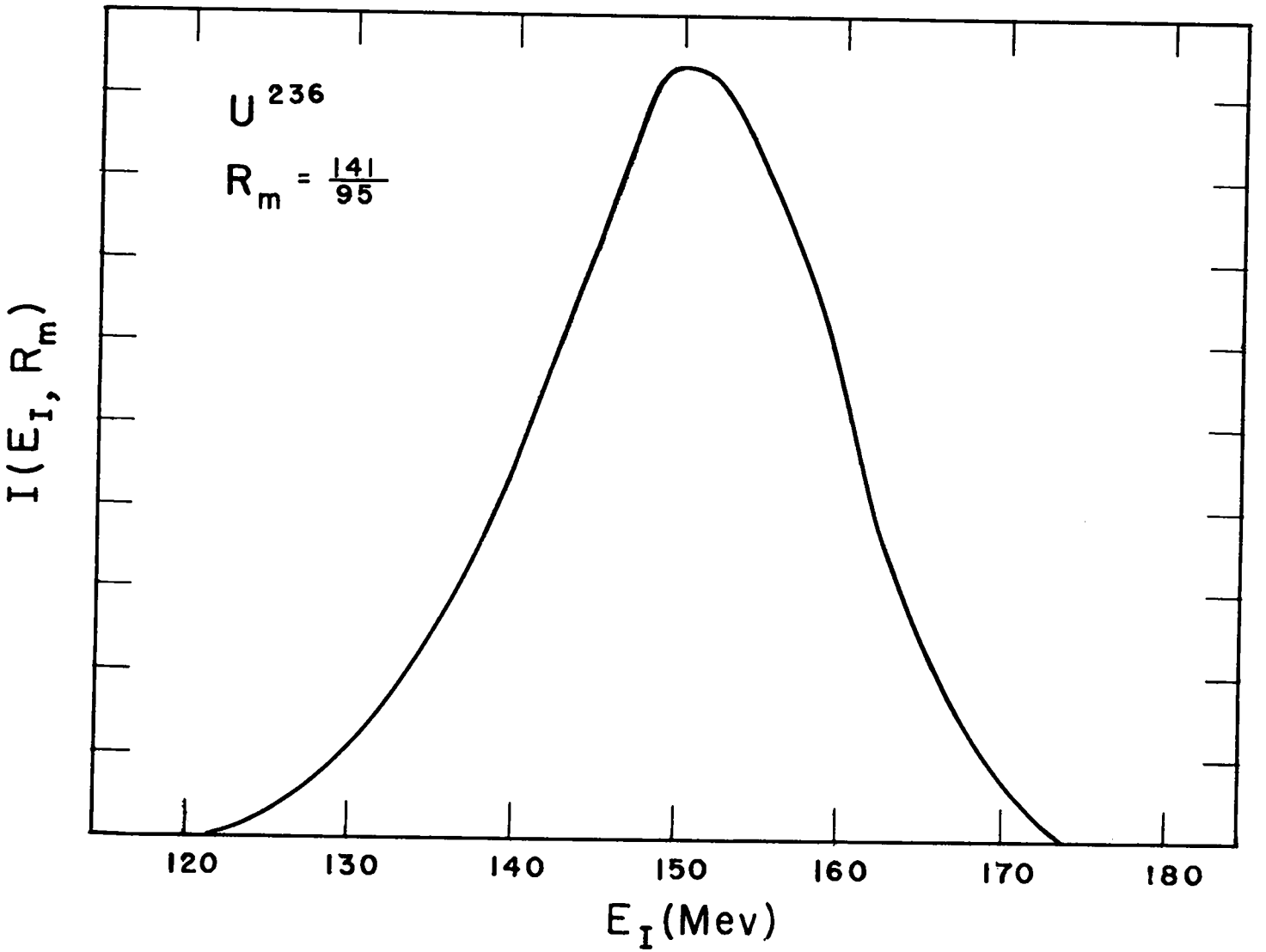


Fig. 3. Ionization energy distribution from Brunton and Hanna.[18] The experimental data are corrected for only the instrumental errors listed by the authors.

APPROVED FOR PUBLIC RELEASE

[redacted]

dispersion obtained from the comparison of mass distributions somewhat more than the dispersion obtained from the comparison of the velocities.

## DISTRIBUTION IN COULOMB ENERGY

In keeping with the assumption of a Coulomb origin of the kinetic energy of fission, the energy distribution $C(E_C, R_m)$ is considered independent of the even-odd term $\delta$. In this way the even-odd term has an effect in the excitation energy of the fission products $E_X$.

The distribution of the energy of fission from ionization chambers is converted into the kinetic energy distribution by the convolution

$$I(E_I, R_m) = \int_{-\infty}^{\infty} dE_C \; C(E_C, R_m) \; D(E_I, E_C) \; . \tag{6}$$

Such an integral equation with the empirical data of $I(E_I, R_m)$ as the solution is difficult to solve exactly. For this reason, an approximate method of solution contained in the Appendix is used throughout this paper. This approximate method involves fitting the empirical $I(E_I, R_m)$ distribution with a series of Gaussian functions. In this manner, all the expressions used in the analysis are Gaussian and thus the solutions of the integral equation 6 and in the integral equation to follow are facilitated.

## DISTRIBUTION IN EXCITATION ENERGY

The distribution $X(E_b, E_X, \delta, R_m)$ in the total excitation energy of fission is obtained by the use of Eq. 1 or 2. This total excitation energy is the excitation energy shared by the fragment pairs of binary fission. However, it is necessary to obtain the excitation energy distributions of the individual fragments $X^L$ and $X^H$ to determine the neutron emission probabilities of fission that are needed.

There exists little experimental evidence on which to decide how the excitation energy $E_X$ is divided into the excitation energies $E_X{}^L$ and $E_X{}^H$ of the individual fission fragments. Consequently, a simple division of excitation energy is used, such that the excitation energies of the individual fragments $X^L$ and $X^H$ are identical distributions of parameters. These parameters are constrained to cause the sum of the excitation energies of the individual fragments to be the total excitation energy. This is to say, if an arbitrary argument $\zeta$ is used, $X^L(\zeta) = X^H(\zeta)$. Under such conditions, the combination of these individual excitation energies into the total excitation energy distribution is given by



[redacted]

[redacted]

$$X(E_b, E_X, \delta, R_m) = \int_{-\infty}^{\infty} dE_X{}^L \int_{-\infty}^{\infty} dE_X{}^H \; X^L(E_b, E_X{}^L, \delta^L, R_m) \; X^H(E_b, E_X{}^H, \delta^H, R_m). \tag{7}$$

The solution of Eq. 7 involves the use of the constraining equation $E_X = E_X{}^L + E_X{}^H$ to yield

$$X(E_b, E_X, \delta, R_m) = \int_{-\infty}^{\infty} dE_X{}^L \; X^L(E_b, E_X{}^L, \delta^L, R_m) \; X^H(E_b, E_X - E_X{}^L, \delta^H, R_m), \tag{8}$$

which is solved by the method in the Appendix.

In Fig. 4 is a typical excitation energy distribution of the individual fragments. It is to be noted that the approximate method of solution leads to impossible negative probabilities of $X(E_X, R_m, E_b, \delta)$ and to impossible negative excitation energies. However, these negative probabilities and energies are preserved throughout the analysis since they do, in a mathematical sense, have meaning.

## EVAPORATION MODEL OF THE NUCLEUS

The evaporation model of the nucleus as formulated by Blatt and Weisskopf[7] involves the use of the square root of the nuclear excitation energy in the exponent in the expression for the neutron emission as a function of the excitation energy. This relation is derived from thermodynamic considerations. However, Blatt and Weisskopf also give the simpler form

$$n(\epsilon)d\epsilon \propto \epsilon \; \exp(-\epsilon/T)d\epsilon, \tag{9}$$

which is shown by Cohen[8] to fit the experimental data satisfactorily. Here $\epsilon$ is the neutron energy in Mev and $n(\epsilon)$ is the probability of emission of a neutron with energy $\epsilon$. This simpler form in Eq. 9 is easier to use in the computations of the emission probabilities $N^L$ and $N^H$ of neutrons. These expressions for the emission probabilities, where $\mu$ is a summation parameter, are



[redacted]

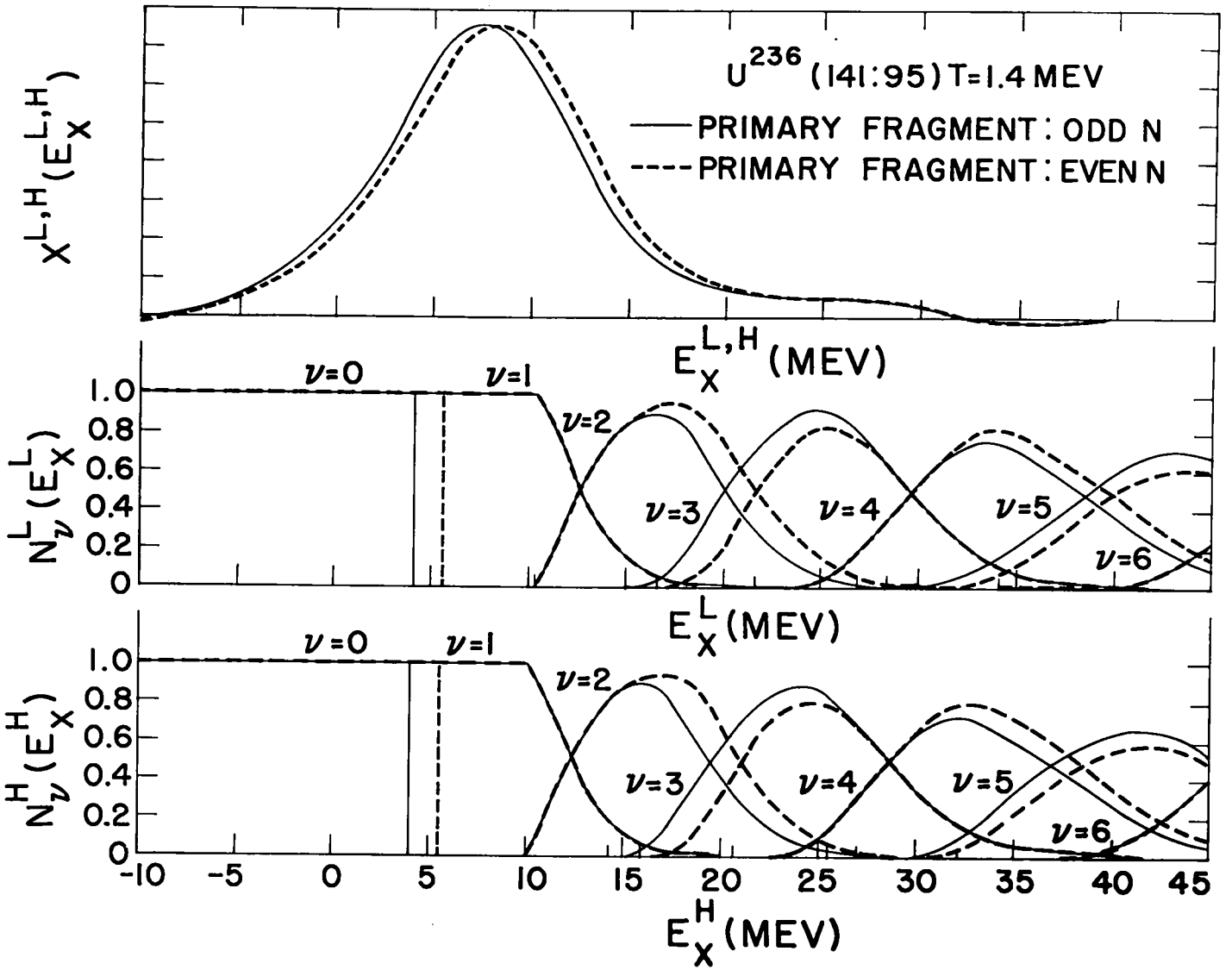


Fig. 4. Excitation energy and neutron emission probabilities calculated for $U^{236}$ fission into the most probable mass ratio. The bias energy $E_b$ is zero in the $X^{L,H}$ case plotted.

[redacted]

$$N_o^L(E_X^L, \delta^L, R_m) = 1 \quad \text{for} \quad E_X^L < B_1^L$$

$$= 0 \quad \text{for} \quad E_X^L \geq B_1^L$$

$$N_1^L(E_X^L, \delta^L, R_m) = 0 \quad \text{for} \quad E_X^L < B_1^L$$

$$= 1 \quad \text{for} \quad B_1^L \leqslant E_X^L < B_2$$

$$\simeq \left\{\left[\exp\left(-\frac{E_X^L - B_2^L}{T}\right)\right]\left[\left(\frac{E_X^L - B_2^L}{T}\right) + 1\right]\right\} \quad \text{for} \quad E_X^L \geq B_2$$

$$N_\nu^L(E_X^L, \delta^L, \nu^L, R_m) = 0 \quad \text{for} \quad E_X^L < B_\nu^L \quad \text{and} \quad \nu > 1$$

$$\simeq \left\{1 - \left[\exp\left(-\frac{E_X^L - B_\nu^L}{T}\right)\right]\left[1 + \sum_{\mu=1}^{2\nu-3} \frac{\left(\frac{E_X^L - B_\nu^L}{T}\right)^\mu}{\mu!}\right]\right\} \qquad (10)$$

$$\text{for } B_\nu^L \leqslant E_X^L < B_{\nu+1}^L \text{ and } \nu > 1$$

$$\simeq \left\{\left[\exp\left(-\frac{E_X^L - B_{\nu+1}^L}{T}\right)\right]\left[1 + \sum_{\mu=1}^{2\nu-1} \frac{\left(\frac{E_X^L - B_{\nu+1}^L}{T}\right)^\mu}{\mu!}\right]\right.$$

$$\left. - \left[\exp\left(-\frac{E_X^L - B_\nu^L}{T}\right)\right]\left[1 + \sum_{\mu=1}^{2\nu-3} \frac{\left(\frac{E_X^L - B_\nu^L}{T}\right)^\mu}{\mu!}\right]\right\}$$

$$\text{for } E_X^L \geqslant B_{\nu+1}^L \text{ and } \nu > 1 .$$

Similar expressions with H superscripts apply for the heavy fragments. Equations 10 are based on Eq. 9 and the assumption that a neutron is always emitted when it is energetically possible.

As has been shown by Cohen, the temperature T appropriate for Eq. 9 is dependent upon the method of excitation of the compound nucleus. It has been suggested by Weisskopf[23] that

[23] V. F. Weisskopf, private communication, 1952.



[redacted]

the temperatures derived by fitting the (n,2n) cross section data[24] with Eq. 10 for nuclides in this mass region are the most appropriate for the use of Eq. 10 in the present calculations. This use of temperatures from (n,2n) data does not involve the uncertainties of the Coulomb barrier in the formation of the compound nucleus. Furthermore, these are temperatures that are derived for excitations of approximately the same magnitude as the most probable excitation of the fission products after fission. The temperatures derived by fitting these (n,2n) data by Eq. 10 are given in Fig. 5. As mentioned before, a question exists about the variation of the nuclear temperature with the neutron-proton ratio for nuclides of a particular mass. However, since the neutron-proton ratio varies only slightly from stable nuclides to those of the neutron-rich fission products, the temperatures in Fig. 5 would not seem to be greatly in error for the fission products. Accordingly, T = 1.4 Mev is used for both the heavy and light fragments for the calculations in this paper.

The binding energies $B^L$ and $B^H$ required in Eq. 10 are computed from the semi-empirical mass surface discussed on page 8. As an illustration of the resulting binding energies, Table I contains those for the most probable mass ratio of the fission yield for fission of $U^{236}$. Although the binding energies of the light fragments are slightly larger than those of the heavy fragments in Table I, the opposite is true for the other two mass ratios used. Also, as discussed above, these binding energies are computed from the part of the semi-empirical mass surface that is three or four charge units from the region of stability and in a region in which few, if any, measurements have been made to check its validity.

TABLE I. NEUTRON BINDING ENERGIES CALCULATED FROM THE SEMI-EMPIRICAL MASS SURFACE

Calculations are for the fission products of $U^{236}$ with a mass ratio $R_m$ = 141/95 and for the most probable (non-integer) nuclear charge. The even-odd term $\delta_2$ represents a primary fission product with an even number of neutrons; $\delta_1$ represents an odd number of neutrons.

| $\nu$ | $B_\nu^L(\delta_1)$ (Mev) | $B_\nu^L(\delta_2)$ (Mev) | $B_\nu^H(\delta_1)$ (Mev) | $B_\nu^H(\delta_2)$ (Mev) |
|---|---|---|---|---|
| 1 | 4.17 | 5.71 | 4.05 | 5.63 |
| 2 | 10.26 | 10.26 | 9.93 | 9.93 |
| 3 | 15.02 | 16.56 | 14.30 | 15.88 |
| 4 | 21.60 | 21.60 | 20.63 | 20.63 |
| 5 | 26.91 | 28.45 | 25.46 | 27.04 |

[24] H. C. Martin and R. F. Taschek, Phys. Rev. 89, 1302 (1953); H. C. Martin and B. C. Diven, Phys. Rev. 86, 565 (1952); and Brolley, Fowler, and Schlacks, Phys. Rev. 88, 618 (1952).

[redacted]

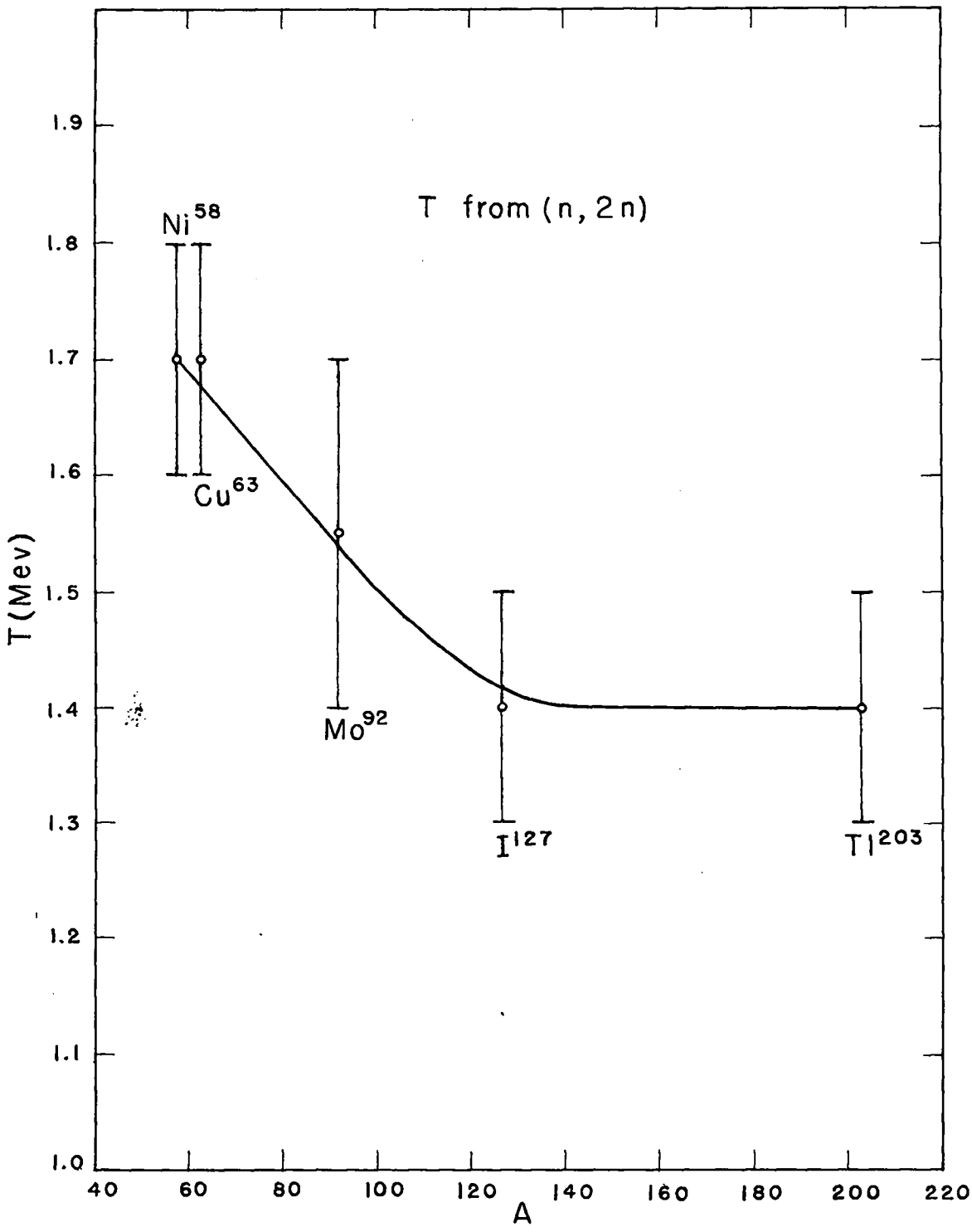


Fig. 5. Temperatures used to fit (n, 2n) data[24] by the evaporation model of neutron emission given in Eqs. 9 and 10.



[redacted]

[redacted]

In Fig. 4 are the $N_\nu^L$ and $N_\nu^H$ distributions from Eq. 10, using the binding energies in Table I, and T = 1.4 Mev. It is to be noted in Table I and in Fig. 4 that both the neutron binding energies and the excitation energy of fission are dependent upon the even-odd character of the fission products.

## NEUTRON EMISSION PROBABILITIES

The neutron emission probabilities as a function of the mass ratio $R_m$ and even-odd parameter $\delta$ are calculated by the use of the integral

$$P_\nu{}^L(E_b, \delta^L, \nu^L, R_m) = \int_{-\infty}^{\infty} X^L(E_b, E_X{}^L, \delta^L, R_m)\ N_\nu{}^L(E_X{}^L, \delta^L, \nu^L, R_m)\, dE_X{}^L. \quad (11)$$

A similar equation for H applies. In practice, Eq. 11 was solved by an IBM 701 by summation over sufficiently wide finite limits, rather than the infinite limits of Eq. 11. The emission probabilities for each value of $\nu^L$ and $\nu^H$ are then combined for all even-odd cases with proper weight for the abundance of each case of $\delta$. Thus, the neutron emission probabilities independent of $\delta$ are obtained. These are written as $P_\nu{}^L(E_b, \nu^L, R_m)$. A similar expression is used for H.

These emission probabilities are for the individual fragments but the needs are for the combined emission probabilities $P_\nu(E_b, \nu, R_m)$ from both fragments of a fission pair. Therefore,

$$P_\nu(E_b, \nu, R_m) = \sum_{\eta=0}^{\nu} P_\eta{}^L(E_b, \nu^L, R_m)\ P_{\nu-\eta}^H(E_b, \nu^H, R_m) \quad (12)$$

is used to form these combined emission probabilities. In Eq. 12, $\eta$ is a summation parameter analogous to $\nu$. Finally, the parameter $R_m$ is removed by combining the emission probabilities with the appropriate weight of the fission probabilities into each region of mass ratio $R_m$. The resulting fission neutron emission probabilities are given in Tables II and III and are discussed further in the following sections.

## RESULTS

The use of the equations discussed above requires data of the fission kinetic energy $E_C$ as a function of the mass ratio of fission. Such data are available[18,19] from double ionization chamber measurements of fission of the compound nuclei $U^{234}$, $U^{236}$, and $Pu^{240}$ and have



[redacted]

TABLE II. CALCULATED EMISSION PROBABILITIES OF NEUTRONS FROM THE COMPOUND NUCLEI UNDERGOING FISSION

The results are approximately normalized to the BNL-250 thermal neutron values $\bar{\nu}(U^{234}) = 2.54 \pm 0.04$, $\bar{\nu}(U^{236}) = 2.46 \pm 0.03$, and $\bar{\nu}(Pu^{240}) = 2.88 \pm 0.04$ by subtracting 5.44 Mev, 2.29 Mev, and 4.78 Mev from the calculated excitation energies of $U^{234}$, $U^{236}$, and $Pu^{240}$, respectively. The effects of (n, n'f) have not been included.

| Compound Nucleus | Energy of Neutron Introducing Fission (Mev) | $\bar{\nu}$ | $P_0$ | $P_1$ | $P_2$ | $P_3$ | $P_4$ | $P_5$ | $P_6$ | $P_7$ | $P_8$ | $P_9$ |
|---|---|---|---|---|---|---|---|---|---|---|---|---|
| $U^{234}$ | (Spontaneous) | | | | | | | | | | | |
| | -6.74 | 1.669 | .1279 | .3192 | .3522 | .1498 | .0523 | .0046 | -.0035 | -.0016 | -.0005 | .0000 |
| | 0 | 2.528 | .0158 | .1295 | .3660 | .3158 | .1354 | .0405 | .0022 | -.0037 | -.0013 | -.0004 |
| | 0.70 | 2.615 | .0121 | .1115 | .3536 | .3296 | .1490 | .0457 | .0040 | -.0038 | -.0014 | -.0004 |
| | 7.00 | 3.365 | .0017 | .0215 | .1853 | .3516 | .2988 | .1132 | .0334 | -.0013 | -.0030 | -.0012 |
| | 14.00 | 4.204 | .0002 | -.0035 | .0428 | .2142 | .3761 | .2557 | .0976 | .0222 | -.0023 | -.0029 |
| $U^{236}$ | (~Spontaneous) | | | | | | | | | | | |
| | -6.50 | 1.676 | .1217 | .3425 | .3256 | .1511 | .0576 | .0071 | -.0033 | -.0017 | -.0006 | -.0001 |
| | -4.00 | 1.974 | .0696 | .2755 | .3621 | .1985 | .0826 | .0176 | -.0025 | -.0022 | -.0009 | -.0002 |
| | -2.00 | 2.215 | .0425 | .2173 | .3683 | .2402 | .1073 | .0291 | -.0004 | -.0027 | -.0012 | -.0003 |
| | 0 | 2.458 | .0250 | .1630 | .3523 | .2810 | .1372 | .0433 | .0034 | -.0031 | -.0016 | -.0004 |
| | 1.00 | 2.581 | .0188 | .1385 | .3368 | .2994 | .1544 | .0516 | .0061 | -.0032 | -.0018 | -.0005 |
| | 4.00 | 2.956 | .0075 | .0780 | .2693 | .3374 | .2140 | .0821 | .0176 | -.0024 | -.0025 | -.0009 |
| | 8.00 | 3.464 | .0017 | .0282 | .1631 | .3291 | .2993 | .1389 | .0418 | .0030 | -.0034 | -.0015 |
| | 14.00 | 4.209 | .0001 | .0014 | .0477 | .2123 | .3566 | .2566 | .1037 | .0255 | -.0010 | -.0031 |
| $Pu^{240}$ | (Spontaneous) | | | | | | | | | | | |
| | -6.30 | 2.083 | .0545 | .2169 | .4095 | .2132 | .1014 | .0157 | -.0041 | -.0049 | -.0018 | -.0004 |
| | -1.50 | 2.681 | .0191 | .1062 | .3118 | .3313 | .1788 | .0585 | .0050 | -.0063 | -.0032 | -.0011 |
| | 0 | 2.889 | .0131 | .0764 | .2660 | .3536 | .2162 | .0750 | .0112 | -.0064 | -.0038 | -.0014 |
| | 7.00 | 3.761 | .0026 | .0041 | .0886 | .2969 | .3888 | .1612 | .0650 | .0015 | -.0053 | -.0033 |
| | 14.00 | 4.556 | .0009 | -.0069 | .0091 | .1481 | .3578 | .3034 | .1503 | .0421 | .0006 | -.0054 |

TABLE III. CALCULATED NEUTRON EMISSION PROBABILITIES FOR FISSION OF NUCLIDES FOR WHICH ADEQUATE FRAGMENT KINETIC ENERGY DISTRIBUTIONS ARE NOT AVAILABLE

Results are not normalized to a measured $\bar{\nu}$ value, but are based on excitation energies 2.29 Mev less than the computed excitation energy. Effects of (n, n'f) have not been included.

| Compound Nucleus | Neutron Energy Inducing Fission (Mev) | $\bar{\nu}$ | $P_0$ | $P_1$ | $P_2$ | $P_3$ | $P_4$ | $P_5$ | $P_6$ | $P_7$ | $P_8$ | $P_9$ |
|---|---|---|---|---|---|---|---|---|---|---|---|---|
| $Th^{233}$ | 2.00 | 1.713 | .1152 | .3305 | .3329 | .1604 | .0586 | .0091 | -.0038 | -.0021 | -.0007 | -.0001 |
| | 14.00 | 3.207 | .0043 | .0507 | .2124 | .3458 | .2557 | .1052 | .0304 | -.0001 | -.0032 | -.0012 |
| $U^{238}$ | {-5.98 Spontaneous} | 2.043 | .0591 | .2542 | .3722 | .2149 | .0854 | .0208 | -.0025 | -.0029 | -.0010 | -.0002 |
| | 2.00 | 3.023 | .0063 | .0678 | .2544 | .3469 | .2226 | .0864 | .0218 | -.0022 | -.0029 | -.0010 |
| $U^{239}$ | 2.00 | 2.672 | .1654 | .1232 | .3169 | .3151 | .1655 | .0586 | .0105 | -.0036 | -.0022 | -.0007 |
| | 14.00 | 4.226 | .0001 | .0023 | .0491 | .2128 | .3494 | .2506 | .1077 | .0303 | .0007 | -.0030 |

been used in the present calculations. However, also of interest are neutron emission probabilities for fission of other compound nuclei for which only single chamber measurements of the kinetic energy have been made.

Calculations have been made for the fission of three such compound nuclei, $U^{238}$ (Ref. 25), $U^{239}$ (Refs. 1, 26), and $Th^{233}$ (Refs. 26, 27). In these cases the variation of kinetic energy with mass ratio obtained from the fission of $U^{236}$ is used with the average energy of fission obtained from the measurements of these nuclei. The binding energy of neutrons to the fission products of these nuclei is computed on the basis of the computed mass surface. In this calculation, the charges of the primary fragments are determined on the basis of the Glendenin[16] hypothesis. The masses are determined on the basis of a fixed heavy fragment mass distribution[14] independent of the mass of the compound nucleus undergoing fission.

In view of the similarity of the kinetic energy distributions for all the nuclei for which double chamber measurements have been made, such a use of the data of both $U^{236}$ and the nuclei in question is expected to give reasonably accurate data. It is, of course, necessary to take into consideration different conditions of the even-odd parameter $\delta$ for the cases of the odd A nuclei $U^{239}$ and $Th^{233}$.

With the approximately 1-Mev uncertainties in the masses used and the approximately 2-Mev uncertainties in the energies used (except for $Th^{233}$, see discussion on page 35), it is not unreasonable to expect an uncertainty of several Mev in the excitation energies derived in the above analysis. Because of this uncertainty, the results of the fission neutron emission calculations for $U^{234}$, $U^{236}$, and $Pu^{239}$ have been normalized to the recent $\bar{\nu}$ measurements[28] of thermal-neutron induced fission, the $\bar{\nu}$ accuracies are about one percent. As indicated in the caption for Table II, this normalization requires a reduction of the calculated excitation energies $E_X$ by several Mev. The close agreement of the amount of this reduction for the three cases indicates that the consistency (from one fissioning nuclide to another) in the mass and energy analysis is accurate to about 3 Mev.

No $\bar{\nu}$ determinations of comparable accuracy for fission of $U^{238}$, $U^{239}$, and $Th^{233}$ are available. Consequently, the 2.29-Mev correction to the excitation energy of the fission of $U^{236}$ is made to apply to these nuclides by the following: The average kinetic energies[25,1,27]

---

[25] W. J. Whitehouse and W. Galbraith, Phil. Mag. 41, 429 (1950).

[26] W. Jentschke, Z. Physik 120, 165 (1943).

[27] J. L. Fowler and L. Rosen, Phys. Rev. 72, 926 (1947).

[28] M. D. Goldberg, J. A. Harvey, D. J. Hughes, and V. E. Pilcher, Brookhaven National Laboratory Report BNL-250, August 1954.

used in these calculations are from measurements which have accompanying $U^{236}$ measurements. Each average $U^{236}$ energy is normalized to that of Brunton and Hanna. The same normalization is then applied to the measurements of $U^{238}$, $U^{239}$, and $Th^{233}$.

It is to be noted in the results in Tables II and III that negative emission probabilities for the larger values of $\nu$ are obtained. Again, these negative probabilities are not physically possible, but have meaning in the mathematical sense. To test whether these negative probabilities have a large influence on the variation of $\overline{\nu}$ and $\overline{\nu^2}$, these quantities were recalculated after dropping the negative probabilities and renormalizing. Although the absolute value of $\overline{\nu}$ and of $\overline{\nu^2}$ for each value of $E_b$ increased by about one percent, the variation of these quantities with $E_b$ changes very little.

It appears from fission cross section measurements as compiled by Barschall and Henkel[29] that the onset for (n,n'f) is between 6 and 7 Mev of incident neutron energy and that the (n,n'f) cross section is of comparable magnitude to the (n,f) cross section up to 14 Mev. The present calculations are only for the (n,f) process, but are adaptable (with reduced accuracy) to the (n,n'f) process by shifting the $E_b$ axis to zero at $E_n \cong 6.5$ Mev. Furthermore, $\nu$ is increased by 1 and the nuclide under consideration changes, for example, from $U^{236}$ to $U^{235}$. It will be seen in the comparison of the results from $U^{239}$ and $U^{238}$ that the neutron emission characteristics of neighboring isotopes are essentially the same.

### (a) Fission of $U^{236}$

Since more experimental data of neutron emission exist for fission of $U^{236}$ than for other nuclides, the fission of this nuclide was investigated most thoroughly in the calculations. In Table IV are the results of the neutron emission calculations for three conditions of temperature and for three conditions of dispersion in the kinetic energy data.

For each parameter, the lower and upper values are considered to be limiting values on the basis of the available data. It is to be noted that changes in the dispersion have considerably less effect on the change of $\overline{\nu}$ and $\overline{\nu^2}$ with $E_n$ than do changes in the nuclear temperature.

In Figs. 6 and 7 are plotted the results from Table II for $\overline{\nu}$ and $\overline{\nu^2}$, respectively. Data in addition to those in Table IV show that the linear relation between $\overline{\nu}$ and $E_n$ in Fig. 4 also applies for the various conditions of T and u discussed above. In Fig. 8 are plotted the results of $P_\nu(E_n)$ of Table II.

[29] H. H. Barschall and R. L. Henkel, LA-1714, August 1954.

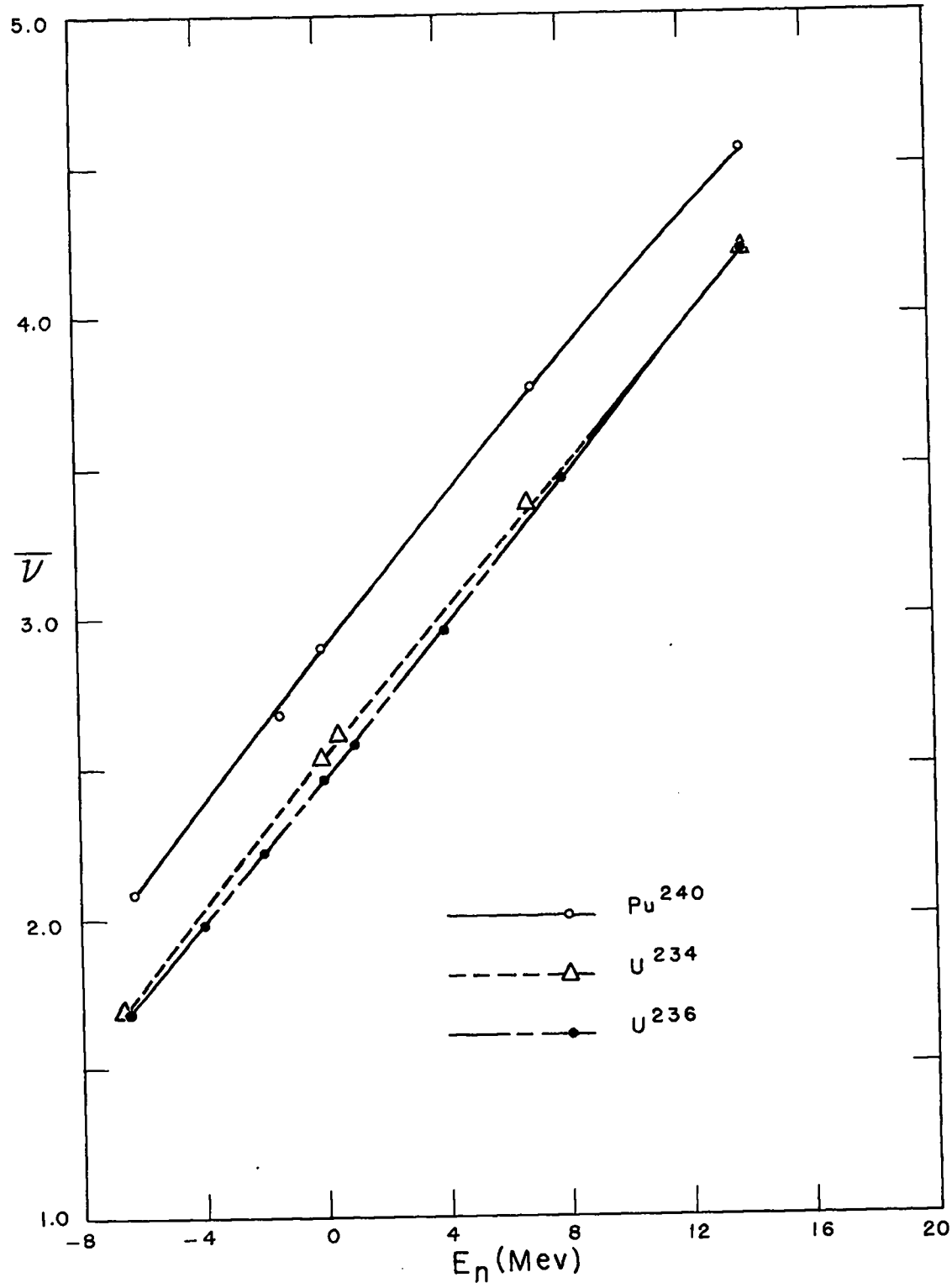


Fig. 6. Plot of the $\overline{\nu}$ data of Table II.

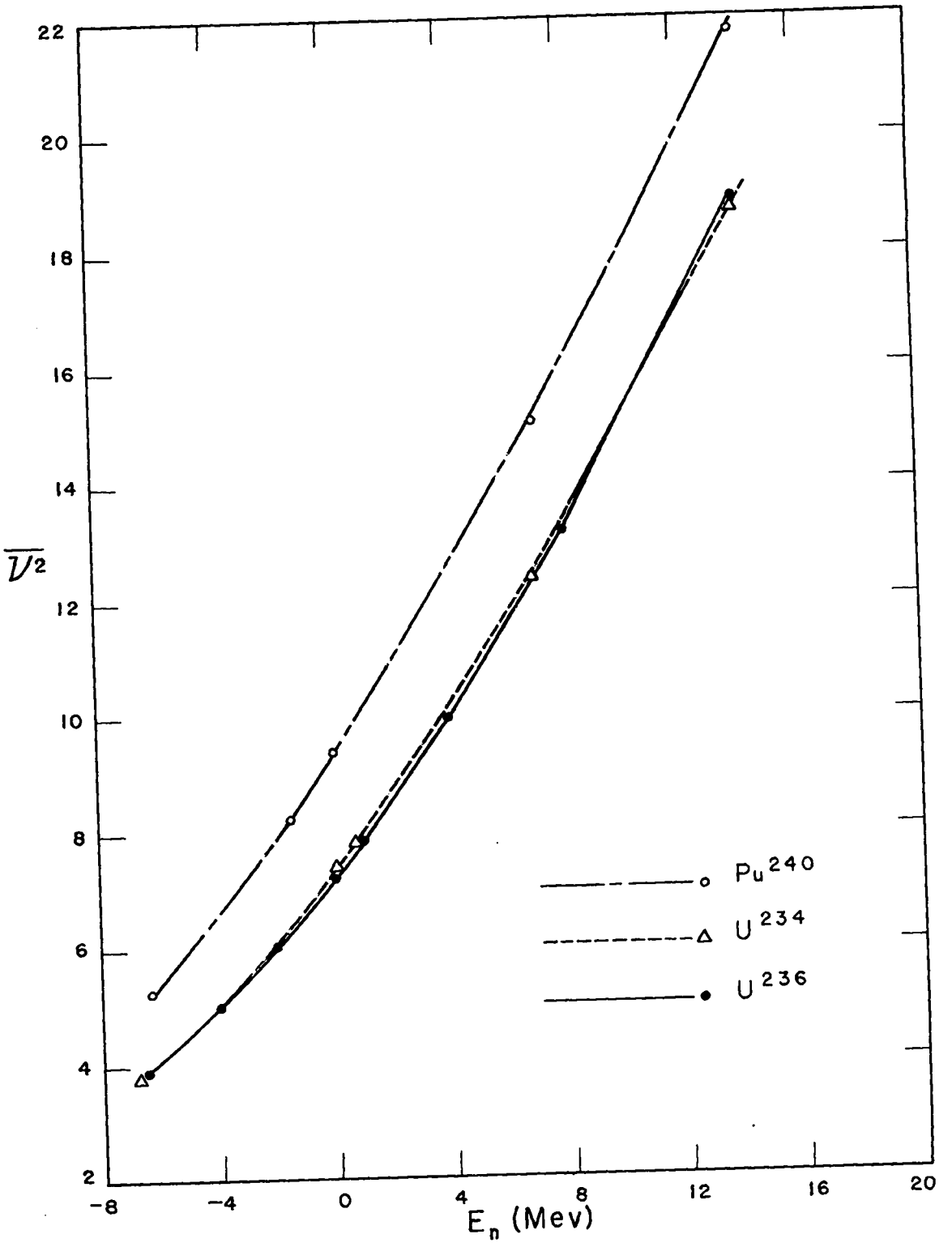


Fig. 7. Plot of the $\overline{\nu^2}$ data obtained from Table II.

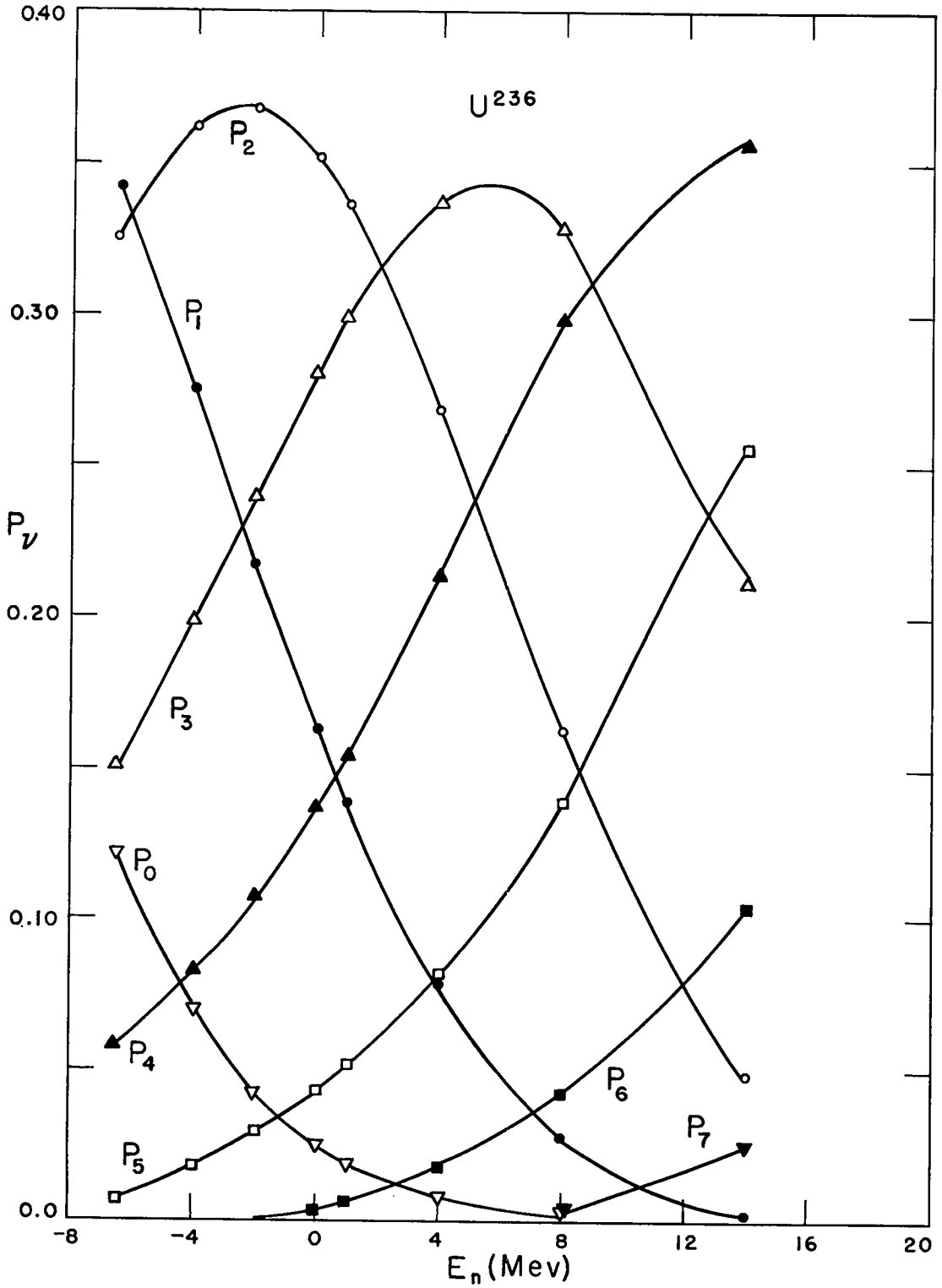


Fig. 8. Plot of the fission neutron emission probabilities of Table II for $U^{236}$ fission.

[redacted]

TABLE IV. DEPENDENCE OF CALCULATED NEUTRON EMISSION PROBABILITIES UPON NUCLEAR TEMPERATURE AND UPON DISPERSION

Calculations are approximately normalized to $\bar{\nu}$ = 2.46 for $E_n$ = 0 by shifting the calculated excitation energy distribution. The parameter u is the width term in the Gaussian expression of the dispersion (Eq. 5). Data are for fission of $U^{236}$.

| T (Mev) | u (Mev) | $E_n$ (Mev) | $\bar{\nu}$ | $\overline{\nu^2}$ | $d\bar{\nu}/dE_n$ ($Mev^{-1}$) |
|---|---|---|---|---|---|
| 1.0 | 7.2 | 0 | 2.4593 | 7.3580 | 0.1468 |
| | | 8 | 3.6341 | 14.7369 | |
| 1.8 | 7.2 | 0 | 2.4648 | 7.1403 | 0.1156 |
| | | 8 | 3.3897 | 12.5834 | |
| 1.4 | 5.9 | 0 | 2.4631 | 7.3567 | 0.1246 |
| | | 8 | 3.4595 | 13.3069 | |
| 1.4 | 8.5 | 0 | 2.4557 | 7.0716 | 0.1263 |
| | | 8 | 3.4661 | 13.1056 | |
| 1.4* | 7.2* | 0 | 2.4581 | 7.2139 | 0.1257 |
| | | 8 | 3.4636 | 13.2096 | |

*Conditions used for other calculations in this report.

(b) Fission of $U^{234}$ and $Pu^{240}$

In Figs. 6 and 7 are the plots of $\bar{\nu}$ and $\overline{\nu^2}$, respectively, for the fission of $U^{234}$ and $Pu^{240}$. These data are in Table II.

(c) Fission of $Th^{233}$, $U^{238}$, and $U^{239}$

In Table III are listed the fission neutron probabilities for the fission of $Th^{233}$, $U^{238}$, and $U^{239}$. As discussed on page 25, these results are not normalized to a $\bar{\nu}$ value, but are based on the same excitation energy correction applied to fission of $U^{236}$.

(d) Effects of (n, n'f)

In Fig. 9 is shown the variation of $\bar{\nu}$ when the effects of (n, n'f) are taken into account, as discussed on page 26. In this analysis it was assumed that the variation of $\bar{\nu}$ as a function of $E_b$ was the same for $U^{234}$ as for $U^{233}$, for $U^{236}$ as for $U^{235}$, and for $Pu^{240}$ as for $Pu^{239}$. This assumption is based upon the results of $U^{238}$ and $U^{239}$ listed in Table III. The difference between the $\bar{\nu}$ results of these two isotopes is satisfactorily explained by the difference in the kinetic energy used in the calculation of these two nuclei. On the basis of the Coulomb origin



[redacted]

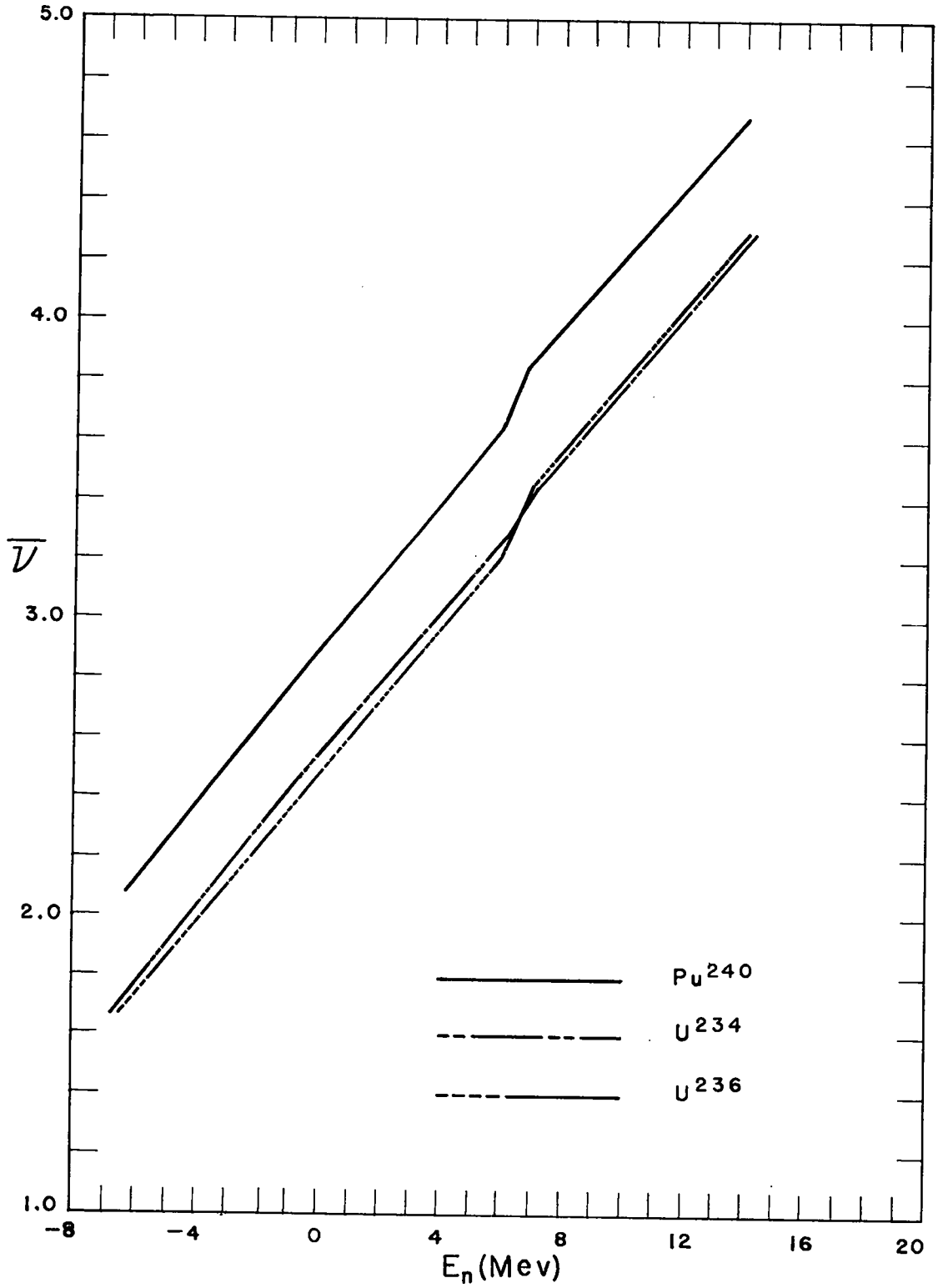


Fig. 9. Plot of $\overline{\nu}$ data of Table II corrected for the effects of (n, n'f).

of the kinetic energy, the same kinetic energy is expected from the two nuclei instead of the measured 3 Mev less for $U^{238}$ compared[25] to $U^{236}$ and 0.7 Mev less for $U^{239}$ compared[1] with $U^{236}$. It is to be noted that the 2.3-Mev difference between the average kinetic energies of $U^{239}$ and $U^{238}$ used in the calculations accounts for 0.30 in $\overline{\nu}$ on the basis of the calculated $d\overline{\nu}/dE_n$. This is to be compared with the 0.35 difference in $\overline{\nu}$ calculated with these masses and energies.

## DISCUSSION

The variation of $\overline{\nu}$ with $E_n$ obtained from these calculations is to be compared with the experimental measurements by sphere multiplication by Graves[30] and Beyster,[31] with the preliminary results from scintillator tank work by Martin et al.,[32] with the chamber measurements by Fowler,[33] and with a combination of counter and radiochemical determinations by Terrell.[34] Similarly, the results of spontaneous fission measurements by Carter[35] and by Segrè[36] for spontaneous fission of $Pu^{240}$ and of Segrè[37] and Littler[38] for $U^{238}$ are to be compared with the calculated results for spontaneous fission. In addition, the liquid scintillation tank has been used by Martin et al.[32] and Hammel and Kephart[39] to obtain preliminary results on the spontaneous fission of $Pu^{240}$. In Table V is a comparison of these experimental results with the present calculated results, and in Table VI is a similar comparison of the $P_\nu$ data.

---

[30] E. R. Graves, LASL P-Division Progress Report, June 20, 1954 (not available).

[31] J. R. Beyster, private communication, 1954.

[32] Martin, Terrell, and Diven, LASL, P-3-76, 1954 and P-Division Progress Report, January 20, 1955 (not available).

[33] J. L. Fowler, Reactor Science and Technology 4, 141 (1954) and Oak Ridge National Laboratory Report ORNL-1715, July 1954.

[34] N. J. Terrell, Jr., Reactor Science and Technology 4, 141 (1954).

[35] W. W. Carter, LA-1582, July 1953.

[36] E. Segrè, LA-491, November 1946.

[37] E. Segrè, Phys. Rev. 86, 21 (1952).

[38] D. J. Littler, Proc. Phys. Soc. London A65, 203 (1952).

[39] J. E. Hammel and J. F. Kephart, as reported in DIR 1003, LASL, 1954 (not available).

[redacted]

TABLE V. COMPARISON OF EXPERIMENTAL AND CALCULATED RESULTS OF AVERAGES OF FISSION NEUTRON EMISSION

The calculated results are of Figs. 7 and 9. Zero energy neutrons and the subscript "th" indicate thermal-neutron induced fission. Effects of (n, n'f) are included.

| Compound Nucleus | Neutron Energy Inducing Fission (Mev) | Quantity | Calculated | Experiment | Experiment Reference |
|---|---|---|---|---|---|
| $U^{236}$ | 1.25 | $\bar{\nu}$ | 2.61 | 2.59 ± .06 | 32 |
| | 4.8 | $\bar{\nu}$ | 3.06 | 3.12 ± .07 | 32 |
| | 4.0 | $\bar{\nu}$ | 2.95 | 3.12 ± 10% | 31 |
| | 4.5 | $\bar{\nu}$ | 3.01 | 3.28 ± 10% | 31 |
| | Fission Spectrum | $\bar{\nu}/\bar{\nu}_{th}$ | 1.10 | 1.05 ± .03 | 31 |
| | 0.7 | $\bar{\nu}/\bar{\nu}_{th}$ | 1.034 | 1.02 ± .02 | 34 |
| | 0.5 | $\bar{\nu}/\bar{\nu}_{th}$ | 1.02 | 1.14 ± .13 | 33 |
| | 2.7 | $\bar{\nu}/\bar{\nu}_{th}$ | 1.13 | 1.42 ± .26 | 33 |
| | 3.7 | $\bar{\nu}/\bar{\nu}_{th}$ | 1.19 | 1.63 ± .23 | 33 |
| | 5.0 | $\bar{\nu}/\bar{\nu}_{th}$ | 1.29 | 1.71 ± .19 | 33 |
| | 14.0 | $\bar{\nu}/\bar{\nu}_{th}$ | 1.79 | 1.99 ± .23 | 33 |
| | 14.0 | $\bar{\nu}$ | 4.29 | 3.95 | 30 |
| $Pu^{240}$ | Spontaneous | $\bar{\nu}$ | 2.08 | 2.20 ± .05 | 32 |
| | Spontaneous | $\bar{\nu}$ | 2.08 | 2.22 ± 5% | 35 |
| | Spontaneous | $\bar{\nu}$ | 2.08 | 2.37 ± .3 | 36 |
| $U^{238}$ | Spontaneous | $\bar{\nu}$ | 2.04 | 2.2 ± .3 | 37 |
| | Spontaneous | $\bar{\nu}$ | 2.04 | 2.5 ± .2 | 38 |
| | Spontaneous | $\overline{\nu^2}/\bar{\nu}$ | 2.57 | 3.26 ± .2 | 40 |
| | Spontaneous | $\overline{\nu^3}/\bar{\nu}$ | 7.28 | 12.73 ± .9 | 40 |
| $U^{239}$ | 1.5 | $\bar{\nu}$ | 2.61 | 2.58 ± .09 | 32 |
| | 4.5 | $\bar{\nu}$ | 2.99 | 3.31 ± ~10% | 31 |
| | 14.0 | $\bar{\nu}$ | 4.30 | 3.5 | 30 |



[redacted]

TABLE VI. COMPARISON OF EXPERIMENTAL AND CALCULATED RESULTS OF PROBABILITIES OF NEUTRON EMISSION $P_\nu$

| Reference | Compound Nucleus | Neutron Energy Inducing Fission (Mev) | $P_0$ | $P_1$ | $P_2$ | $P_3$ | $P_4$ | $P_5$ | $P_6$ | $P_7$ |
|---|---|---|---|---|---|---|---|---|---|---|
| 32 | $U^{236}$ | 0.08 | .014 | .165 | .357 | .306 | .115 | .046 | -.006 | -.002 |
| | | | ±.005 | ±.016 | ±.022 | ±.024 | ±.020 | ±.013 | ±.005 | ±.002 |
| Calc. | $U^{236}$ | 0 | .025 | .163 | .352 | .281 | .137 | .043 | .003 | -.003 |
| 32 | $Pu^{240}$ | Spontaneous | .050 | .215 | .352 | .263 | .110 | .013 | -.005 | .003 |
| | | | ±.009 | ±.021 | ±.029 | ±.031 | ±.026 | ±.015 | ±.008 | ±.004 |
| 39 | $Pu^{240}$ | Spontaneous | .008 | .26 | .42 | .15 | .11 | .05 | -- | -- |
| Calc. | $Pu^{240}$ | Spontaneous | .055 | .217 | .410 | .213 | .101 | .016 | -.004 | -.005 |

The calculated increase of $\bar{\nu}$ with $E_n$ is seen from Table V to be very close to the measured increase, perhaps being somewhat larger than the measured increase. As seen by Table IV, the difference between the 14-Mev values of Graves compared with the calculated values in Table V and, similarly, the corresponding spontaneous fission values for $Pu^{240}$, can probably be explained on the basis of temperature or dispersion alone. As an alternative explanation, these differences can possibly be explained by a true mass surface in the region of the fission products that is less steep than predicted by the parabolic surface used.

The calculated results of $\bar{\nu}$ and $\overline{\nu^2}$ for $U^{236}$ in Figs. 6 and 7, respectively, were integrated over the fission neutron spectrum and the resulting values for fission neutron induced fission are $\bar{\nu} = 2.70$ and $\overline{\nu^2} = 8.48$.

Multiplicity measurements have been made by counter techniques for spontaneous fission of $U^{238}$ by Geiger.[40] It is to be noted in Table V that satisfactory agreements between most of the more recent experimental data and the calculated data exist, but the multiplicity measurements of Geiger are somewhat larger than the present calculated results. This discrepancy can be partially explained by the apparently incorrect normalization for the $U^{238}$ data, as evidenced by the low calculated results of $\bar{\nu}$ of spontaneous fission of $U^{238}$ compared with the experimental value. Such a possibility of the calculated $\bar{\nu}$ being low is, however, difficult to explain on the basis of the energies used in the calculation. As discussed on page 32, the measured kinetic energy of fission used in the calculations is about 3 Mev less than the anticipated Coulomb energy and thus the calculated $\bar{\nu}$ is about 0.36 greater than what would be obtained if the "true" Coulomb energy were used in the calculations.

Of all the calculated results, those of the compound nucleus $Th^{233}$ are most uncertain. As seen in Table III, the use of the $E_C$ values of Fowler and Rosen[27] in the calculations yields surprisingly low values of $\bar{\nu}$. These 1947 data of Fowler and Rosen[27] were used in preference to the 1943 data of Jentschke[26] as being more recent. However, a surprisingly large discrepancy exists between these two sets of experimental data when each is normalized to the accompanying $U^{236}$ measurements. Fowler and Rosen find 2.6 Mev less energy for $Th^{233}$ than $U^{236}$ while Jentschke finds 9.5 Mev less. On the basis of the calculated $d\bar{\nu}/dE_n$, $\bar{\nu}$ values 0.85 greater than those of Table III would be obtained if the data of Jentschke were used. In view of these large discrepancies for $Th^{233}$, the results for $Th^{233}$ are considered to be of less accuracy than the other data.

The present calculations can also be used to determine the neutron emission probabilities from the several mass groups of the fission products used in the calculations. These results are contained in Table VII. It is seen that no correlation of $\bar{\nu}$ with $R_m$ can be determined

[40] K. W. Geiger and D. C. Rose, Can. J. Phys. 32, 498 (1954).

with certainty. This is in contrast to the radiochemical determinations,[15] which indicate that $\bar{\nu}$ is lower for $R_m$ values near unity than for larger $R_m$ values. Thus, radiochemical determinations indicate a relatively smaller probability of neutron emission from the fragments in the symmetrical fission region. It should be emphasized that the $E_C$ data for the low and high $R_m$ values for each fission case are of relatively low accuracy compared with the $E_C$ data of the most probable mass ratio value. This is because of poorer statistics and the effects of dispersion.[4] As a result, the $\bar{\nu}$ values calculated for these low and high $R_m$ values are subject to error.

TABLE VII. CALCULATED NEUTRON EMISSION PROBABILITIES OF VARIOUS GROUPS

These data correspond to thermal-neutron induced fission when the calculated excitation energies are normalized as in Table II. Mass ratios are the center of each of the three mass ratio groups. The results for all mass ratio groups (properly weighted) are referred to as "all."

| Compound Nucleus | Mass Ratio | $\bar{\nu}^L$ | $\bar{\nu}^H$ | $\bar{\nu}$ | $\bar{\nu}^L/\bar{\nu}^H$ |
|---|---|---|---|---|---|
| $U^{234}$ | 133/101 | 0.828 | 0.695 | 1.539 | |
| | 141/93 | 1.218 | 1.286 | 2.504 | |
| | 149/85 | 2.475 | 2.365 | 4.839 | |
| | All | 1.328 | 1.327 | 2.655 | 1.001 |
| $U^{236}$ | 131/103 | 1.440 | 1.152 | 2.592 | |
| | 141/95 | 1.212 | 1.244 | 2.456 | |
| | 149/87 | 1.045 | 0.970 | 2.015 | |
| | All | 1.248 | 1.185 | 2.433 | 1.053 |
| $Pu^{240}$ | 131/109 | 1.341 | 1.105 | 2.446 | |
| | 139/101 | 1.523 | 1.607 | 3.131 | |
| | 147/93 | 1.458 | 1.453 | 2.912 | |
| | All | 1.449 | 1.410 | 2.859 | 1.027 |

It is of interest to compare the calculated $\bar{\nu}^L/\bar{\nu}^H$ values of Table VII with the measured values found by Fraser[41] by the angular correlation of fragments and neutrons in a coincidence

[41] J. S. Fraser, Phys. Rev. 88, 536 (1952).

[redacted]

experiment. Fraser found $\overline{\nu^L}/\overline{\nu^H}$ to be 1.30 ± 0.08 for fission of the compound nuclei $U^{234}$, $U^{236}$, and $Pu^{240}$. The corresponding ratios 1.00, 1.05, and 1.03 in Table VII indicate that the assumed equality of the excitation energy distributions $X^L$ and $X^H$ of the light and heavy fragments is in error and, instead, larger excitation energies of the light fragments should be used. On the other hand, the theory of fission proposed by Fong[4] predicts $\overline{\nu^L}/\overline{\nu^H} < 1$.

In later work on $U^{234}$ with similar techniques, Fraser and Milton[42] found $\overline{\nu}$ to be greatest for the most probable fission mode and to decrease 10 to 20 percent for symmetrical and approximately symmetrical fission modes. In addition, they found, for both the light and heavy fragments, an increase of $\overline{\nu^L}$ or $\overline{\nu^H}$ with mass of the fragment. As discussed above, the uncertainties of the $E_C$ data for the less probable fission modes makes the corresponding data of Table IV unsuitable for comparison.

In addition to the data compared in Table V, two other determinations of $\overline{\nu}$ can be compared. Wahl[43] used the observed nuclear charge distribution of the fission products from 14-Mev neutron induced fission of the compound nucleus $U^{236}$ and the Glendenin hypothesis[16] of the nuclear charge of fission fragments and obtained a value of $\overline{\nu}$ = 5.2 ± 0.5 for 14-Mev neutron fission of the compound nucleus $U^{236}$. Using the same method with the same nuclide, Ford[44] found $\overline{\nu}$ = 3.1 for $E_n$ = 5 Mev and $\overline{\nu}$ = 4.8 for $E_n$ = 14 Mev. An analysis of recent sphere measurements with various energy neutrons inducing fission of the compound nucleus $U^{236}$ has been made by Goad.[45] She finds the data fit best by $\overline{\nu}$ = 2.5 for $E_n < 3.9$ Mev, $\overline{\nu}$ = 3.0 for 3.9 Mev $< E_n <$ 6.5 Mev, and $\overline{\nu}$ = 3.5 for $E_n > 6.5$. Because of the less direct determinations of these values, they have not been included in Table V, even though the agreements with the present calculated results are reasonable.

---

[42] J. S. Fraser and J. C. D. Milton, Phys. Rev. 93, 818 (1954).

[43] J. S. Wahl, LAB-P-4 Memo, 1952 (not available).

[44] G. P. Ford, private communication, 1952.

[45] M. S. Goad, T-602, 1954, and revisions of this (not available).



[redacted]

[redacted]

## APPENDIX

This appendix describes the method of solution of the integral equations 6 and 8 involving the empirical data of $I(E_I, R_m)$.

For convenience, the transposition of the $E_I$ data by the 12.4-Mev ionization defect is first made by a replotting of the $I(E_I)$ data into $I'(E_I')$ data, where $E_I'$ is $E_I' = E_I + 12.4$. With such a transposition of the original data, a transposition by the dispersion function is not necessary. The dispersion is thus redefined by

$$D'(E_C, E_I') \propto \exp\left[-\left(\frac{E_C - E_I'}{u}\right)^2\right], \tag{13}$$

where u is the width of the dispersion.

In the approximate method, it is assumed that $I'(E_I')$ can be fit adequately well by a series of Gaussian functions so that

$$I'(E_I') = \sum_{\beta=0}^{12} b_\beta \exp\left[-\left(\frac{E_I' - E_o + \beta d}{w}\right)^2\right], \tag{14}$$

where $b_\beta$ terms are amplitude coefficients, $\beta$ is a summation parameter, $E_o$ is an energy constant, d is the spacing of the Gaussians, and w is the width term of the Gaussians. In Eq. 14 and the analysis to follow, the parameters $R_m$ and $\delta$ are not written because the analysis applies for any condition of $R_m$ and $\delta$.

Since the $I'(E_I')$ data are fit by Eq. 14, a limited freedom of choice of the values of the $E_o$, w, and d terms exists. In practice, the solutions of the equations to follow were facilitated by the following choices: The width w is slightly less than the width of the $I'(E_I')$ distribution to be fitted, d is roughly 0.8 w, and $E_o = (E_I')_{max} + 7d$. The most probable $E_I'$ is $(E_I')_{max}$. With the 13-Gaussian system used, these choices result in the seventh Gaussian as the dominant term and the other Gaussians tailor this curve to fit the empirical $I'(E_I')$ data.

Two Gaussian expressions can be shown to fold as



[redacted]

[redacted]

$$\exp\left[-\left(\frac{E_I' - E_o + \beta d}{w}\right)^2\right] \propto \int_{-\infty}^{\infty} dE_C \left\{\exp\left[-\left(\frac{E_C - E_o + \beta d}{v}\right)^2\right]\right\}\left\{\exp\left[-\left(\frac{E_C - E_I'}{u}\right)^2\right]\right\} \tag{15}$$

where $w^2 = v^2 + u^2$. Thus, a substitution of the fitted $I'(E_I')$ expression of Eq. 14 into the convolution (Eq. 6) is,

$$\sum_{\beta=0}^{12} b_\beta \exp\left[-\left(\frac{E_I' - E_o + \beta d}{w}\right)^2\right] \tag{16}$$

$$\propto \int_{-\infty}^{\infty} dE_C \left\{\sum_{\beta=0}^{12} b_\beta \exp\left[-\left(\frac{E_C - E_o + \beta d}{v}\right)^2\right]\right\} \left\{\exp\left[-\left(\frac{E_C - E_I'}{u}\right)^2\right]\right\} .$$

From Eqs. 16 and 6, the fitted Coulomb energy distribution is seen to be

$$C(E_C) = \sum_{\beta=0}^{12} b_\beta \exp\left[-\left(\frac{E_C - E_o + \beta d}{v}\right)^2\right] , \tag{17}$$

where $w^2 = v^2 + u^2$ and v is the width of the Gaussian terms fitting $C(E_C)$.

The transformation from Coulomb energy $E_C$ to the total excitation energy of the fragment pairs $E_X$ is by Eq. 2. Thus, with $E_C = \phi - E_X$, the excitation energy distribution is written

$$X(E_X) = \sum_{\beta=0}^{12} b_\beta \exp\left[-\left(\frac{\phi - E_o - E_X + \beta d}{v}\right)^2\right] . \tag{18}$$

It is now required to find the excitation energy distributions of the individual fragments. As discussed in the text, these are considered identical, such that $X^L = X^H$, and are combined by

$$X(E_X) = \int_{-\infty}^{\infty} dE_X{}^L \, X^L(E_X{}^L) \, X^H(E_X - E_X{}^L) . \tag{8a}$$

The substitution of $X(E_X)$ of Eq. 18 into Eq. 8a gives



[redacted]

[redacted]

$$\sum_{\beta=0}^{12} b_\beta \exp\left[-\left(\frac{\phi - E_o - E_X + \beta d}{v}\right)^2\right] = \int_{-\infty}^{\infty} dE_X{}^L \, X^L(E_X{}^L) \, X^H(E_X - E_X{}^L) \, . \tag{19}$$

It can be shown that Eq. 19 and $X^L = X^H$ are satisfied by

$$\sum_{\beta=0}^{12} b_\beta \exp\left[-\left(\frac{\phi - E_o - E_X + \beta d}{v}\right)^2\right]$$

$$= \int_{-\infty}^{\infty} dE_X{}^L \left\{ \sum_{\alpha=0}^{6} a_\alpha \exp\left[-\left(\frac{\frac{\phi - E_o}{2} - E_X{}^L + \alpha d}{v/\sqrt{2}}\right)^2\right]\right\}$$

$$\times \left\{ \sum_{\alpha=0}^{6} a_\alpha \exp\left[-\left(\frac{\frac{\phi - E_o}{2} - E_X + E_X{}^L + \alpha d}{v/\sqrt{2}}\right)^2\right]\right\}, \tag{20}$$

if the following conditions between the amplitude parameters $b_\beta$ and $a_\alpha$ are satisfied:

$$\begin{aligned}
b_0 &= a_0{}^2 \\
b_1 &= 2\, a_0 a_1 \\
b_2 &= 2\, a_0 a_2 + a_1{}^2 \\
b_3 &= 2\, a_0 a_3 + 2\, a_1\, a_2 \\
b_4 &= 2\, a_0 a_4 + 2\, a_1\, a_3 + a_2{}^2 \\
b_5 &= 2\, a_0 a_5 + 2\, a_1\, a_4 + 2\, a_2 a_3 \\
b_6 &= 2\, a_0 a_6 + 2\, a_1 a_5 + 2\, a_2 a_4 + a_3{}^2 \\
b_7 &= 2\, a_1 a_6 + 2\, a_2 a_5 + 2\, a_3 a_4 \\
b_8 &= 2\, a_2 a_6 + 2\, a_3 a_5 + a_4{}^2 \\
b_9 &= 2\, a_3 a_6 + 2\, a_4 a_5 \\
b_{10} &= 2\, a_4 a_6 + a_5{}^2 \\
b_{11} &= 2\, a_5 a_6 \\
b_{12} &= a_6{}^2 \, .
\end{aligned} \tag{21}$$



[redacted]

[redacted]

When these conditions are satisfied the excitation energy distributions of the individual fragments are found as

$$X^{L}(E_X{}^{L}) = \sum_{\alpha=0}^{6} a_\alpha \exp\left[-\left(\frac{\frac{\phi - E_o}{2} - E_X{}^{L} + \alpha d}{v/\sqrt{2}}\right)^2\right] \qquad (22)$$

and the corresponding equation for the heavy fragment. Again, $w^2 = v^2 + u^2$.

It is now necessary to use the conditions given in Eqs. 21 with the fit of the $I'(E_I')$ experical data by Eq. 14 to solve for the $a_\alpha$ amplitude parameters required in the $X^L$ and $X^H$ expressions of Eq. 22. Equations 21 are a set of 13 simultaneous equations that are quadratic in $a_\alpha$ terms. To solve for the $a_\alpha$ values, the 13 expressions for the 13 $b_\beta$ terms in Eqs. 21 are substituted in the equation of the fit to the empirical data, which is Eq. 14. The resulting 13 simultaneous equations, each of which is a quadratic of $a_\alpha$ terms multiplied by a Gaussian expression, are to be solved at 13 empirical values of $I'(E_I')$.

The method used for this solution was to take as the 13 values of $I'(E_o')$ the values at $E_I' = E_o$, $E_I' = E_o - d$, $E_I' = E_o - 2d$, .... $E_I' = E_o - 12d$. Under these conditions and the previously stated conditions that result in $b_6$ being dominant, these 13 simultaneous, quadratic equations are solved by an iterative method. The first solution is assumed to be $a_3 = 1$ and $a_0 = a_1 = a_2 = a_4 = a_5 = a_6 = 0$. With this solution substituted, the resulting inequality in the fourth equation is used to find $a_0$, the inequality in the fifth equation to find $a_1$, the sixth for $a_2$, the eighth for $a_4$, the ninth for $a_5$, and the tenth for $a_6$. These solutions of $a_\alpha$ are substituted and the same corrections are applied. The process is repeated many times. The resulting fits of the empirical $I'(E_I')$ data are given in Table VIII.



[redacted]

TABLE VIII. PARAMETERS FOUND TO FIT THE EMPIRICAL $E_I'$ DATA

The $a_\alpha$ values are relative to $a_3 = 1.00$ and are not absolute.

| Compound Nucleus | $R_m$ | w (Mev) | d (Mev) | $E_o$ (Mev) | $a_0$ | $a_1$ | $a_2$ | $a_3$ | $a_4$ | $a_5$ | $a_6$ |
|---|---|---|---|---|---|---|---|---|---|---|---|
| $U^{234}$ | 133/101 | 11.40 | 9.0 | 223 | -.020 | -.012 | .196 | 1.000 | .069 | .170 | -.105 |
| | 141/93 | 11.40 | 9.0 | 217 | .019 | -.048 | .068 | 1.000 | .016 | .061 | -.037 |
| | 149/85 | 9.48 | 7.5 | 201 | .238 | -.486 | .642 | 1.000 | .335 | -.077 | .006 |
| $U^{236}$ | 133/103 | 13.80 | 11.0 | 241 | -.001 | -.011 | .039 | 1.000 | .066 | .088 | -.034 |
| | 141/95 | 11.40 | 9.0 | 220.5 | .010 | -.041 | .120 | 1.000 | .046 | .066 | .028 |
| | 149/87 | 9.48 | 7.5 | 204 | -.022 | .009 | .127 | 1.000 | .081 | .069 | -.042 |
| $Pu^{240}$ | 131/109 | 13.80 | 11.0 | 245 | .060 | -.161 | .339 | 1.000 | .136 | .129 | -.009 |
| | 139/101 | 11.40 | 9.0 | 226 | .101 | -.228 | .341 | 1.000 | .074 | .098 | -.040 |
| | 147/93 | 9.48 | 7.5 | 209 | -.029 | .023 | .120 | 1.000 | .015 | .090 | -.038 |